Journal of
Materials Chemistry B

Accepted Manuscript

This article can be cited before page numbers have been issued, to do this please use: Z. Gu, R. Zhou, S. Zhu, L. Gong, Y. Fu and Y. zhao, *J. Mater. Chem. B*, 2019, DOI: 10.1039/C8TB03240H.

ROYAL SOCIETY OF CHEMISTRY

rsc.li/materials-b

View Article Online
DOI: 10.1039/C8TB03240H

Journal Name

ARTICLE

Recent advance of stimuli-responsive systems based on transition metal dichalcogenides for smart cancer therapy

Received
Accepted

DOI:

www.rsc.org/

Ruxin Zhou[a,b,#], Shuang Zhu[a,#], Linji Gong[a,b], Yanyan Fu[*d], Zhanjun Gu[*a,b] and Yuliang Zhao[a,b,c]

Stimuli-responsive systems, which can be used for temporally and spatially controllable therapeutic platforms, have been widely investigated in cancer therapy. Among a wide range of stimuli-responsive nanomaterials, transition metal dichalcogenides (TMDCs) have recently attracted great attention due to their large surface-to-volume ratio, atomic thickness, and other unique physicochemical properties. Thus, TMDCs are able to be responsive to various endogenous (e.g. acidic pH and overexpressed enzymes) or exogenous stimuli (e.g. light and magnetic). The majority of TMDC-based therapeutic platforms are triggered by near-infrared (NIR) light. However, due to the limited penetration of NIR light, novel strategies that are able to ablate deep-sited tumor tissues have emerged in recent years and have been applied to design multi-stimuli-responsive nano-systems. A comprehensive overview of the development of stimuli-responsive TMDC-based nanoplatforms for "smart" cancer therapy is presented to demonstrate a more intelligent and better controllable therapeutic strategy. Furthermore, the versatile properties of TMDCs and the typical responsive principles of certain stimuli-responsive platforms are discussed for a better understanding of selected examples in this review.

1. Introduction

Stimuli-responsive systems (or named "smart" systems), have attracted great attention in the field of cancer therapy in recent years. It is characterized by the spatial-, temporal- and dosage-controlled fashion. Compared with conventional therapeutic systems, the most significant advantage of the "smart" platform is the on-demand process, which is also termed as "switch on/off".[1] Thus, it can overcome the limitations in previously reported therapeutic systems and can increase the longevity and stability of the carrier *in vivo*, specifically target pathological organs or tissues in the body, release drugs or genes in a temporally and spatially controllable manner, and avoid undesired accumulation in the healthy tissues.[2-5]

Interests in stimuli-responsive nano-systems have been persisted over several decades. Currently, many nanomaterials have been utilized, such as nano-graphene, liposomes, polymeric micelles, polymeric nanoparticles, dendrimers, inorganic nanoparticles, and many others.[6-8] These nanomaterials can be specifically modified in response to certain intrinsic characteristics of pathological tissues or external stimuli applied from the outside of the body.[7] These stimuli can be employed for three main functions. Firstly, it can induce a controllable release of drug/gene cargo from nanomaterials. Taken drug delivery system (DDS) as an example, once exposed to exogenous (*e.g.* light and magnetic) or endogenous stimuli (*e.g.* acidic pH and overexpressed enzymes), it switches on certain functions. Drug release can be controlled by the changes in physicochemical properties, such as carrier degradation or an increase in the permeability, or by the cleavage of chemical bonds used to attach the drug to the carrier. Thus, such stimuli-responsive DDS can deliver drugs only where and when they are needed, at the right concentration. The main advantage of these systems is to minimize drug exposure and side effects at sites where the drug/gene is not needed.[7,9-12] The next two applications are always derived from external stimuli. It can provide direct therapeutic effects, such as photothermal therapy (PTT) and radiotherapy (RT). Furthermore, it can be used for bioimaging application.[13] Since imaging plays a significant role in diagnosis, treatment, and confirmation of therapy, such stimuli-responsive platform can be used for development of cancer theranostic systems to enhance the therapeutic efficiency, monitor the particle biodistribution and therapy response.[14]

Among various nanomaterials applied in stimuli-responsive platforms, transition metal dichalcogenide (TMDC), an emerging inorganic analogue of graphene, has attracted an increasing number of interests during recent years. TMDCs are

[a] *CAS Key Laboratory for Biomedical Effects of Nanomaterials and Nanosafety, Institute of High Energy Physics, Chinese Academy of Sciences, Beijing 100049, China*
**E-mail: zjgu@ihep.ac.cn*
[b] *College of Materials Science and Optoelectronic Technology, University of Chinese Academy of Sciences, Beijing 100049, China*
[c] *CAS Center for Excellence in Nanoscience, National Center for Nanoscience and Technology of China, Chinese Academy of Sciences, Beijing 100190, China*
[d] *State Key Lab of Transducer Technology, Shanghai Institute of Microsystem and Information Technology, Chinese Academy of Sciences, Changning Road 865, Shanghai 200050, P. R. China. *E-mail: fuyy@mail.sim.ac.cn*
 # The authors contributed equally to this work.

semiconductors of the type MX_2, where M is a transition metal from group 4 to 10 in the periodic table (*e.g.* Mo, W, Ti) and X represents a chalcogen atom (*e.g.* S, Se, Te).[15] Due to the unique electronic structures, TMDC nanomaterials possess some specific properties and could be used in "smart" therapeutic systems and many other fields.[16-19] Firstly, TMDCs often crystallize in a layered structure with a hexagonally packed layer of metal atoms sandwiched between two layers of chalcogen atoms. The intralayer M–X bonds are covalent, while the sandwich layers are interacted by weak van der Waals forces.[20] Thus mono- or fewer-layered TMDCs are relatively easy to be exfoliated from bulk materials. Secondly, TMDCs are easy to be surface functionalized and thus the potential applications of TMDCs in different environments will be broadened.[17] If the anchored molecules carry additional groups which are sensitive to a specific stimulus, the TMDC-based material can be affected by the stimulus, change its physicochemical properties and lead to specific cancer therapy. Besides, two dimensional (2D) TMDC nanosheets (NSs), with large surface-to-volume ratios, can be used in DDSs to load a large number of chemotherapeutic drugs, biomolecules, and functional molecules.[21,22] Furthermore, many TMDCs have high absorption coefficient in the near-infrared (NIR) region (650–900 nm).[23] They also have a salient photothermal effect, and thus could convert light into thermal energy with high efficiency. Therefore, TMDCs have great potential to be applied in PTT and photoacoustic (PA) imaging.[24-27] In addition, compared to many other nanostructures, TMDCs induce fewer cytotoxic responses and are much less hazardous, thus favouring its biological applications.[28] As a result, stimuli-responsive DDSs based on nano-carriers, especially TMDC nanomaterials have been increasingly developed and reported in recent years.[10]

Though the applications of TMDC-based cancer theranostic systems have been summarized for several years,[17,19,22,29] an article that generally covered the development of stimuli-responsive TMDC-based nanoplatforms for "smart" cancer therapy is still rare. With more stimuli being applied into one platform, the system became increasingly intelligent and more controllable. Therefore, this review is aimed at giving a relatively comprehensive overview of some representative rational designs and progress of TMDC-based nanomaterials for stimuli-responsive drug delivery and cancer therapy, and proposing current challenges and future perspectives in this field.

2. Design of TMDC-Based Smart Platforms

2.1. Attributes of TMDC to Design Smart Platforms

The proof-of-principle design of TMDC-based stimuli-responsive systems is to combine TMDC or its derivatives with other specific moieties into a single system. Thus, the unique physicochemical properties of TMDC and its derivatives may affect the stimuli-responsive or drug loading/release performances. The details are described as follows.

(1) **Surface Functional Groups.** By changing the surface chemistry, the biocompatibility, sensitivity as a diagnostic tool, dispersity and stability of original materials can be improved.[29] Surface functionalization is one of the strategies. The recent construction of stimuli-responsive DDSs is based on nanomaterials followed by targeting functionalization, bioconjugation and surface modification. The large surface-to-volume ratio of TMDC nanomaterial makes it easy to be modified with specific polymers and surfactants to improve the therapeutic efficiency and broaden the range of the applications. By controlling the synthetic method, encapsulation approach and the functional groups, the as-synthesized therapeutic platform can show in-demand manners, and thus the stimuli-responsive performance can be affected.[30] For example, the strong coordination interaction between carboxyl groups of PEG and tungsten atoms improves the stability of WS_2 in water and physiological solutions. In addition, by modifying the materials with mesoporous silica (MS), the drug could be loaded inside MS shell, improving the efficiency of drug delivery. Besides, by modifying TMDC or its derivatives with targeting moieties, including FA, peptides and materials with strong magnetic property (*e.g.* Gd chelator, Fe_3O_4), the targeting ability can be improved, leading to a better drug loading/release performance controlled by various external and internal stimuli.

(2) **Dimension**. From 3D to 2D, due to the decrease in dimensionality, the interlayer coupling, degree of quantum confinement, and symmetry elements will change. Thus, some properties of bulk materials are preserved and several novel physicochemical characteristics may appear.[16,31]

Compared to the bulk material with an indirect bandgap of ~1eV, the mono-layer 2D TMDC material with the same composition has a direct bandgap due to quantum confinement effects. Additionally, the prismatic edges and basal planes are exposed and free the adjacent MX_2 layers from s-p_z orbital interaction, leading to a wider bandgap. These changes in the band structure result in enhanced photoluminescence in 2D TMDC.[16] Besides, 2D TMDC materials have a larger surface-to-volume ratio. On the one hand, monolayer TMDC materials are more sensitive to environmental factors and thus possess low carrier mobility.[15] On the other hand, it makes 2D TMDC materials easier to be covalently functionalized and provides maximal interaction not only with the targeted biomaterials, increasing the sensitivity of the specific stimulus in tumor microenvironment, but also with chemotherapeutic drugs, enhancing therapeutic efficiency. Thus, 2D TMDC with a structure similar to that of graphene has attracted an increasing number of interests in the recent years.

Further decreasing the dimensionality to zero, zero-dimensional (0D) TMDC nanodots (NDs) or quantum dots (QDs) with ultrasmall size possess stronger quantum confinements, more edge atoms, photoluminescence properties and better biocompatibility compared to multi- and mono-layer TMDC nanomaterials. Hence, 0D TMDC NDs or QDs have emerged as a promising type of biomedical nanomaterials.[32,33]

(3) **Size**. Another way of controlling the surface chemistry is size control. To minimize the side effect of the biomedicines, the hydrodynamic size of them should be controlled under the threshold of kidney filtration (<10 nm) so that these nanomaterials could be excreted through the kidney in short time through the renal-clearance pathway.[33,34] In addition, a smaller size causes low-coordination step-edges, kinks and corner atoms which can

View Article Online DOI: 10.1039/C8TB03240H

induce additional chemical effects.[16] Therefore the development of ultrasmall TMDC NDs can further improve the therapeutic efficiency and performances of the bulk and few- to mono-layer TMDC nanomaterials.

(4) **Composition**. The chemical composition of TMDCs, especially the metal atom is another important factor that can influence the stimuli-responsive performance. The transition metal atom provides four electrons to bond with chalcogen atoms so that the coordination environment of the transition metal and its *d*-electron count has a significant effect on the electronic structure of TMDCs. Furthermore, it causes various electronic and magnetic properties, improving the drug loading/release performance.[16]

2.2. Stimuli for Design of TMDC-Based Smart Platforms

Recently, due to their unique structures and distinctive properties mentioned above, TMDC nanomaterials have attracted more and more interests in the biomedical field, and have been widely investigated in drug delivery, PTT, photodynamic therapy (PDT) and RT applications. In addition, the easy-functionalization of TMDC can endow these materials with adaptive features and thus smart systems in responsive to both endogenous and exogenous stimuli can be designed based on these materials.

2.2.1 Endogenous Stimuli

Endogenous stimuli have been increasingly considered to design "smart" DDSs. Since tumor microenvironment (TME) is a complex system and possesses various distinctive features, such stimuli-responsive nano-systems can target TME and/or intracellular components to realize on-demand accumulation and release of drugs. These physiological signals mainly include tumor and endocytic acidity, redox potential (glutathione, GSH), specific enzyme overexpression, hypoxia, and adenosine-5'-triphosphate (ATP).[2,35]

pH Level: Among the endogenous biological stimuli, pH is a ubiquitous one that has been widely used to develop novel and responsive DDSs for cancer therapy. The extracellular and intracellular environment of tumors is considered more acidic than normal tissues. In general, the pH values in healthy tissues and blood maintain around 7.4, while the extracellular pH values in the tumors range from 6.0 to 7.2. Furthermore, the intracellular value of tumors can even decrease to 4.0–6.0.[2] Such striking acidosis at TME is mainly a consequence of irregular angiogenesis in fast-growing tumors. It can lead to a rapid deficiency of oxygen and thus a shift towards a glycolytic metabolism, essentially causing the production of acidic metabolites in the tumor site.[1,35-37] pH-responsive TMDC-based nano-carriers are often functionalized with polymers to deliver drugs. It can be divided into two main strategies. The first one includes polymeric systems with acid-sensitive bonds, such as the hydrazine linkage that possesses excellent pH sensitivity. Upon reaching the mildly acidic environment, the bonds will cleave and enable the release of molecules anchored at the surface of TMDCs. Another strategy is to use polymers (polyacids or polybases) with ionizable functional groups, whose conformation and/or solubility changes in accordance with the environmental pH values.[1,38] As a result, the drug release is inhibited during systemic circulation at the physiological pH value of about 7.4 and is only allowed in the acidic environment at cancer cells.[39] Thus, the pH gradient is an effective stimulus for TMDC-based therapeutic platforms.

GSH: Redox state directly decides on many cellular processes. By capturing the energy released in oxidation processes, cellular and organismic structures can be built and the balance of life can be maintained.[40] Many redox couples work together to maintain the redox environment, among which the glutathione disulfide (GSSG)/GSH couple is one of the most abundant couples.[41-43] GSH, a γ-glutamyl-cysteinyl-glycine tripeptide, plays a role of the main reducing agent to facilitate the thiol-disulfide exchange reaction.[7,44] It has been found that in order to protect the cells from reactive oxygen species (ROS), the concentrations of GSH in some highly reducing intracellular milieu (*e.g.* cytosol, mitochondria, and cell nucleus) are 2–10 mmol L^{-1}, extremely higher than those in the blood or extracellular matrices (2–20 μmol L^{-1}). [2,6,35,45] Since the tumor tissue was highly reducing and hypoxic, the concentration of GSH is more than 4 times higher than that of normal tissue, and the significant difference of GSH level between the normal and tumor cells makes GSH a promising stimulus for redox-mediated drug delivery.[46] The construction of GSH-responsive platforms based on TMDC nanomaterials mainly utilized an S–S bridge where chemotherapeutic drugs could be linked or physically entrapped. In the presence of GSH, the S–S bridge breaks up and converts to thiols (–SH HS–), while GSH itself is oxidized to GSSG.[46] As a result, the drugs could be dumped into the malignant cells *via* GSH-responsive nano-vehicles and this targeted intracellular drug release approach could significantly enhance the drug efficacy, overcome drug resistance, and reduce side effects.[46-48]

Enzymes: Enzymes, often over-expressed in disease states, are indispensable in cell regulation and can accelerate the kinetics of most biochemical reactions.[40,49] Based on their mechanisms, enzymes can be divided into six types, including oxidoreductases, transferases, hydrolases, lyases, isomerases, and ligases.[50] The overexpression of some enzymes in cancerous cells can be utilized in enzyme-responsive DDSs. Enzyme-sensitive moieties can be covalently attached to the surface of TMDC *via* the formation of specific bonds. Then the high enzyme concentration in tumor sites is able to catalyse the delivery vector such that it degrades, changes the shape or structure, or breaks the bond, thus resulting in the specific drug release.[50] The most closely cancer-related enzymes are metalloproteinases, cathepsin B and hyaluronidase (HAase), which are promising stimuli to improve the efficacy of cancer killing.[40,51,52]

Hypoxia: Hypoxia, defined as reduced O_2 level, is a major hallmark of tumors. It plays an important role in tumor angiogenesis, metastasis, and multidrug resistance.[53] The oxygen concentration in many solid tumors is about 4% and it can be even non-measurable in some local tumor environments.[54,55] The low oxygen tension has many negative effects. For example, it causes resistance to the current applied antitumor therapeutics, such as chemotherapy, PDT, and RT, since the efficacy of these strategies strongly depends on the level of tumor oxygen supply.[53] To enhance the therapeutic efficiency, numerous attempts have been focused on hypoxia-triggered activation of therapeutic systems. Tumor cells consumed large quantities of nutrients and oxygen, resulting in the imbalance between oxygen supply and consumption, while blood vessels around tumors are not able to give enough oxygen.[35,56,57]

View Article Online
DOI: 10.1039/C8TB03240H

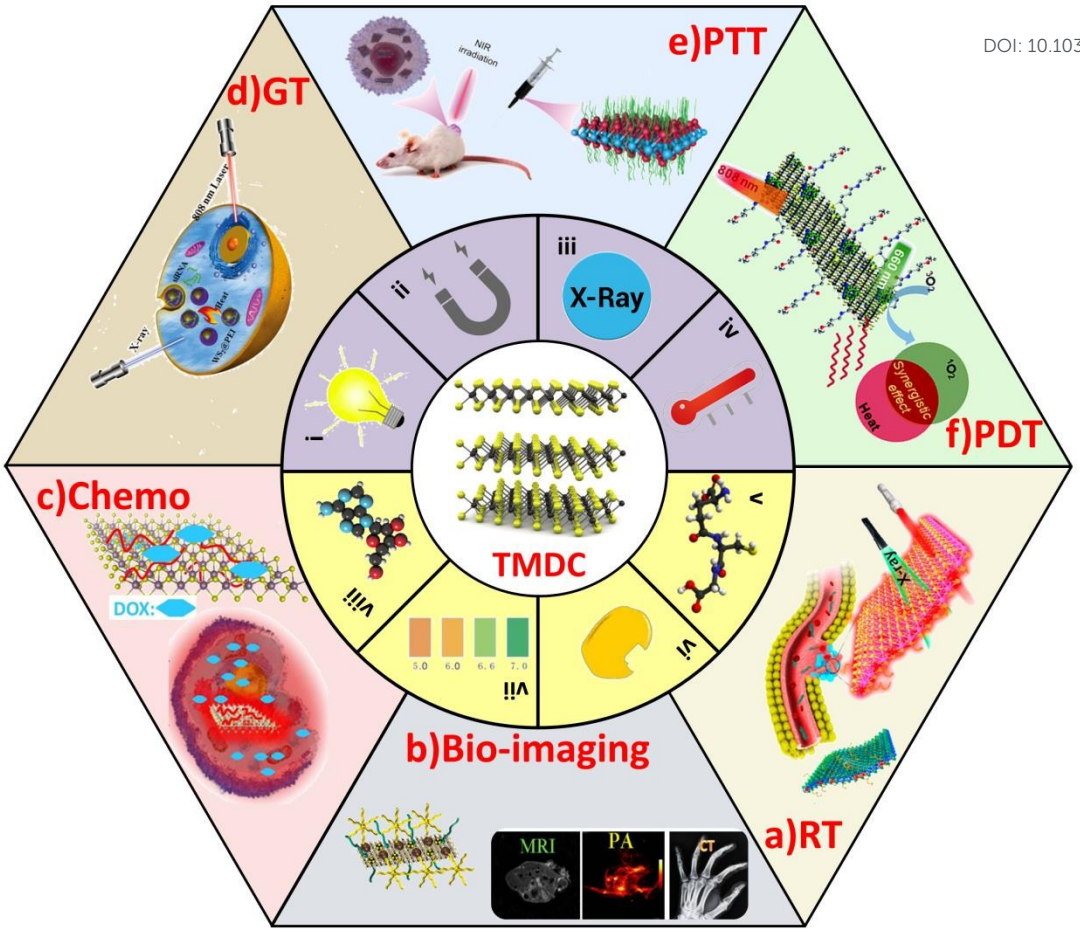

Fig.1 Schematic of a variety of stimuli to trigger the release of drugs or directly induce therapeutic effects based on transition metal dichalcogenides for combined therapy: (i) light; (ii) magnetic field; (iii) X-ray; (iv) temperature; (v) GSH; (vi) enzyme; (vii) pH level; and (viii) other biomolecules, e.g. ATP. (a: Adapted from ref. 167, Copyright 2015, American Chemical Society; b: Adapted from ref. 96, Copyright 2016, Dove Medical Press Limited; c: Adapted from ref. 108, Copyright 2014, The Royal Society of Chemistry; d: Adapted from ref. 123 Copyright 2016, John Wiley and Sons; e: Adapted from ref. 107, Copyright 2014, American Chemical Society; f: Adapted from ref. 13 Copyright 2015, American Chemical Society; Adapted from ref. 20 Copyright 2011, Springer Nature. Reproduced with permission.)

Thus, the gradient of oxygen concentration can be utilized in both diagnosis and treatment of cancer.[58,59] Nano-carriers composed of hypoxia-responsive moieties (*e.g.* nitrobenzyl alcohols, nitroimidazoles, and azo linkers), have been applied in DDSs for tumor ablation.[60] However, so far, the TMDC-based cancer therapeutic platforms sensitive to hypoxia have not been reported yet. Consequently, this new strategy is worth taking into account to design and fabricate TMDC-based drug carrier, which is beneficial to promote the therapeutic effects.

Other Biomolecules: Another promising approach that can selectively target malignant cells over healthy ones is based on the overexpression of specific biomolecules on the malignant cells, such as membrane proteins (*e.g.* folic acid (FA) receptors, hyaluronic acid (HA) receptors, transferrin (Tf) receptors).[45,61-65] Besides, ATP, the energy source of cells, can be functioned as an internal stimulus as well. ATP has higher intracellular concentration compared with the extracellular environment. Synthetic ATP aptamers or proteins, with the covalent attachment of chemotherapeutic drugs, can fall off the surface of functionalized TMDC nanomaterials because of the strong affinity with target molecules. Therefore, the drug can be delivered and released in a targeted manner.[45,66]

2.2.2 Exogenous Stimuli

Compared with internal stimuli related to the microenvironment of cancer, external stimuli are more reliable and efficient because they can control the activation and release of the loaded cargoes more precisely.[45] The primary principles of DDS responsive to external stimuli are similar to those of internal stimuli: upon exposing to exterior stimuli, their physicochemical properties will be changed, which further induces the release of payloads or activation of prodrugs in a controllable way.[67] Besides, some exogenous stimuli, like light and magnetic field, can not only be utilized to develop smart stimuli-responsive systems, but also induce additional therapeutic and imaging effects. Other exogenous stimuli including microwave (MW) and radiation are also widely integrated with functionalized TMDC nanomaterials for cancer therapy.

Light: Light was known as an outstanding external stimulus due to its non-invasive nature and spatial and temporal control over the release of cargo even in the distance.[10,68] Since NIR light can penetrate deeper, the main source of light in TMDC studies is NIR laser. As we mentioned above, TMDC nanomaterials have strong absorbance ability in the NIR region (650–900 nm) and a salient photothermal effect.[17,69,70] Thus they can be used as photothermal

agents for PTT, generating heat under NIR irradiation and directly killing cancer cells.[6] The photo-responsive groups can be encapsulated within, or conjugated to the surface of the nano-system.[7,71] Then considering the ability of TMDC materials to carry massive photosensitizers (PSs), the temperature elevation can also be used to trigger PSs to produce enormous ROS, thus stimulating PDT.[72,73] Similarly, therapeutic drugs and genes can also be applied on the surface of TMDCs and once irradiated by NIR laser, the cargoes will be released at a specific site for irreversible ablation of cancer cells.

Magnetic Field: Magnetic field has been widely used as an exogenous stimulus in biomedical applications to enhance magnetic resonance imaging (MRI) contrast, control the release of therapeutic agents, and conduct magnetic field-assisted radionuclide therapy.[7,74] TMDC-based materials hybridized with magnetic nanoparticles, such as superparamagnetic iron oxide (SPIO) nanoparticles (*e.g.* maghemite (γ-Fe_2O_3) and magnetite (Fe_3O_4)),[75-77] can be magnetically controlled, and concentrated at the pathological site (tumors).[68,78,79] Thus, drugs can be released from the carriers at the particular location, for more efficient and accurate ablation of cancer cells. In addition, gadolinium (Gd)-functionalized TMDCs or some of TMDC materials themselves (*e.g.* vanadium disulfide (VS_2)) can be used to produce a positive MR contrast.[80,81] Another application of magnetic nanoparticles is tumor hyperthermia therapy due to its capability to induce magnetic fluid hyperthermia (41–43 ℃) and cause damages to tumors.[6] Taken together, magnetic stimulus can be employed for the delivery and targeted release of drug molecules, bioimaging (MRI), and hyperthermia therapy.[45] Moreover, compared to optical-dependent therapy, magnetic fields, particularly with frequencies below 400 Hz, have no penetration limitation in bio-tissue, making remote implementation without physical contacts possible.[66,67]

X-ray: X-ray radiation is a stimulus that has been widely applied in RT. According to the mechanism, RT could be divided into two main types, external-beam radiation therapy (EBRT) and internal radioisotope therapy (IRT). Nanomaterials containing high-*Z* elements are usually employed for EBRT, because they could absorb ionizing-radiation beams and then result in the generation of secondary charged particles and the enhancement of cancer cell death. However, the corresponding radioactive agents of IRT are generally administrated or implanted into the body to irradiate tumor sites from the inside for cancer treatment.[17,82-84] TMDC nanomaterials, with high-*Z* elements, can be used as radiosensitizers for both EBRT and IRT. Upon exposing to radiation, it can kill cancer cells and improve the efficacy of RT.[85] Besides, due to its strong X-ray attenuation ability, TMDCs have great potential to play the role of contrast agents in computed tomography (CT) imaging.

Microwave: Microwave, with a longer penetration depth, faster heat generation, shorter irradiation durations, larger ablation zones and less susceptibility to local heat sinks, is another exogenous stimulus.[86] It can be used to generate heat *via* MW susceptible agents which have spatial confinement microcapsule walls, such as TMDC nanomaterials. When the pathological site is heated, hyperthermia is able to inhibit synthesis of DNA, alter protein synthesis, disrupt microtubule organizing centres, change the expression of receptors and ultimately, change the cellular morphology.[7,11,87] Therefore, MW is a promising candidate for the facilitation of forthcoming therapeutic platforms to trigger internal temperature change, control the release of drugs and irreversibly ablate tumors.

3. NIR light triggered multi-stimuli-responsive platform based on TMDC for cancer therapy

Due to their electronic band structure, TMDC nanomaterials, with strong optical absorption in NIR region and high photothermal conversion efficiency,[15] have been widely used in light-responsive cancer therapy such as PTT,[88-96] controlled drug release[24,26,97-102] or PDT[103,104]. Compared to visible light, NIR light of 650–900 nm can realize deeper tissue penetration and be less absorbed by biological tissues, and it thus can achieve better therapeutic effects.[23,93]

The photo-responsive research based on MoS_2 originated from PTT application (Fig. 2) and the first attempt was conducted by Chou and co-workers.[105] They synthesized chemically exfoliated MoS_2 ($ceMoS_2$) nanomaterials and applied it as NIR photothermal agent due to its superior photothermal characteristic. The photothermal killing of cancer cells has been confirmed *in vitro* at the cell culture level. $ceMoS_2$, with the mass extinction coefficient (λ = 800 nm, 29.2 L g^{-1} cm^{-1}), displayed approximately 7.8 times greater absorbance in the NIR light compared to that of nano-GO (3.6 L g^{-1} cm^{-1}). To explore the *in vivo* applications, Cheng *et al.* designed surface functionalized TMDCs to examine therapeutic effects in animals.[106] The obtained polyethylene glycol (PEG)-coated WS_2 (WS_2-PEG) exhibited good biocompatibility and appeared to be a powerful PTT agent. It was found that after being either intratumorally or intravenously injected with WS_2-PEG into mice, the tumor surface temperature rose from ~30 ℃ to ~65 ℃ within five-minute NIR laser irradiation. Furthermore, experiments on Balb/c mice uncovered 100% of tumor elimination by either intratumoral (i.t.) injection (2 mg kg^{-1}) or intravenous (i.v.) injection (20 mg kg^{-1}) of WS_2-PEG under the exposure of 808 nm-NIR laser at a relatively low power density, without recurrence during the subsequent 45 days.

Considering the ultra-high surface area, TMDCs could be loaded with PSs, genes, nitric oxide (NO) and chemotherapeutic drugs with high loading capacity.[29] Under the laser irradiation, the heat transformed from the light energy by TMDC, on the one hand, could trigger drug release from the surface. On the other hand, it could enhance the uptake of drugs since the permeability of cell membrane is increased by the heat.[107-109] Therefore, the TMDC mediated mild photothermal heating could realize the enhancement of drug uptake in cellular environment, the remote control of drug release and minimal side effects to normal tissues.[6] Thus, with strong NIR absorbance, TMDCs have demonstrated great potential to act as nano-carriers at light-responsive DDSs.

For example, TMDCs have been used as photosensitizer carriers for the design and fabrication of a "smart" PDT system.[110-115] In a work conducted by Yong *et al.*, WS_2 NSs were used to deliver methylene blue (MB, one of PSs) due to their high surface area.[104] Moreover, the PDT effect could be finely controlled by NIR laser,

View Article Online
DOI: 10.1039/C8TB03240H

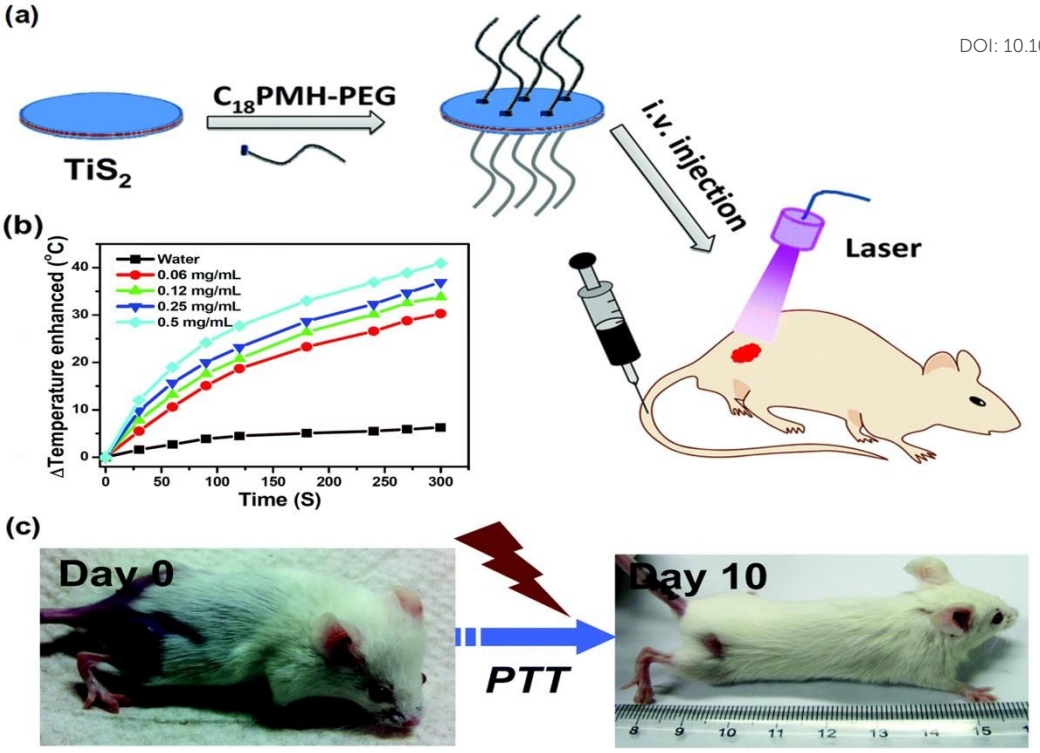

Fig.2 Two-dimensional TiS_2 nanosheets for *in vivo* photoacoustic imaging and photothermal cancer therapy. (a) Schematic illustration of using TiS_2-PEG nanosheets for photoacoustic imaging guided photothermal therapy. (b) Photothermal heating curves of pure water and TiS_2-PEG solutions with different concentrations (0.06, 0.12, 0.25, and 0.5 mg mL^{-1}) under 808 nm laser irradiation at a power density of 0.8 W cm^{-2}. (c) *In vivo* photothermal therapy: Photographs of tumor-bearing mice with i.v. injection of TiS_2-PEG (12 h post injection) before laser irradiation (left) and 10 days after photothermal treatment (right). (Adapted from ref. 94, Copyright 2015, The Royal Society of Chemistry. Reproduced with permission.)

which could regulate the release of MB from the surface of WS_2 NSs. During delivery process, due to the high light absorbance of WS_2 and efficient energy transfer from MB to WS_2, singlet oxygen ($^1O_2$) generation of MB would be highly quenched by WS_2, and thus the PDT effect was mostly inhibited. When the nanoparticles reached tumor sites, the photoactivity of PSs could be recovered by NIR irradiation. The heat generated from TMDC by NIR irradiation could disturb the interaction between WS_2 NSs and MB, and cause efficient release of MB, which recovered the production of $^1O_2$ and then killed the cancer cells efficiently. The above-mentioned features made it a smart PDT platform and could dramatically improve PDT selectivity in tumors and reduce side effects on normal tissues. *In vitro* experiment showed only 20% cell viability of HeLa cells with BSA-WS_2@MB, 665 nm LED lamp and 808 nm laser, significantly lower than any other groups. Thus, the as-synthesized WS_2 NSs could not only load PSs, but also regulate the generation of singlet oxygen by NIR irradiation, realizing a smart NIR-responsive therapeutic platform and increasing the accuracy and efficacy for cancer therapy. In another work conducted by Liu and co-workers, PEGylated MoS_2 NSs were prepared and loaded with chlorin e6 (Ce6), another photodynamic agent, *via* supramolecular "π-π" stacking.[108] In this nanoplatform, once irradiated by NIR laser, Ce6 would transfer the photon energy to molecular oxygen to generate $^1O_2$ and kill nearby cancer cells.[110-113] Moreover, it has also been found that NIR-light triggered mild hyperthermia was capable to increase cell membrane permeability, promote cellular uptake of various agents and improve photodynamic cancer cell killing efficiency.[116] Taking advantage of these properties, tumor growth in mice i.v. injected with MoS_2-PEG/Ce6, irradiated with both 606 nm light (PDT) and 808 nm laser (PTT) was significantly inhibited compared to any other groups. Thus, after combining these two representative phototherapeutic methods, PDT and PTT, a superadditive therapeutic effect could be realized.

Apart from PSs, TMDC nanomaterials are also widely used in stimuli-responsive gene delivery for gene therapy (GT). Gene therapy, namely, is associated with the delivery of genetic materials, like small interfering RNA (siRNA) molecules.[117-123] It treats diseases by directly transferring genetic material into the cancer cells themselves to cause destruction, or indirectly, either by stimulating the immune system for the recognition and elimination of the cancer cells or by targeting the non-malignant stromal cells that support the growth and metastasis of cancer cells.[124] Compared to chemotherapy, gene therapy can overcome several difficulties, such as the intrinsic drug resistance and drug dosage limitation, thus offering opportunities to obtain a more specific therapeutic platform.[45,125] In addition, gene therapy could also be used to inhibit the expression of the genes related to the heat shock response triggered by PTT, and thus improved the PTT therapeutic effect. Based on the enhanced efficiency of combined therapy, Kim *et al.* designed a gene delivery system with single-layered MoS_2-PEI-PEG nanocomposites, responsive to both NIR light and GSH.[126] It is well documented that GSH plays a significant role in

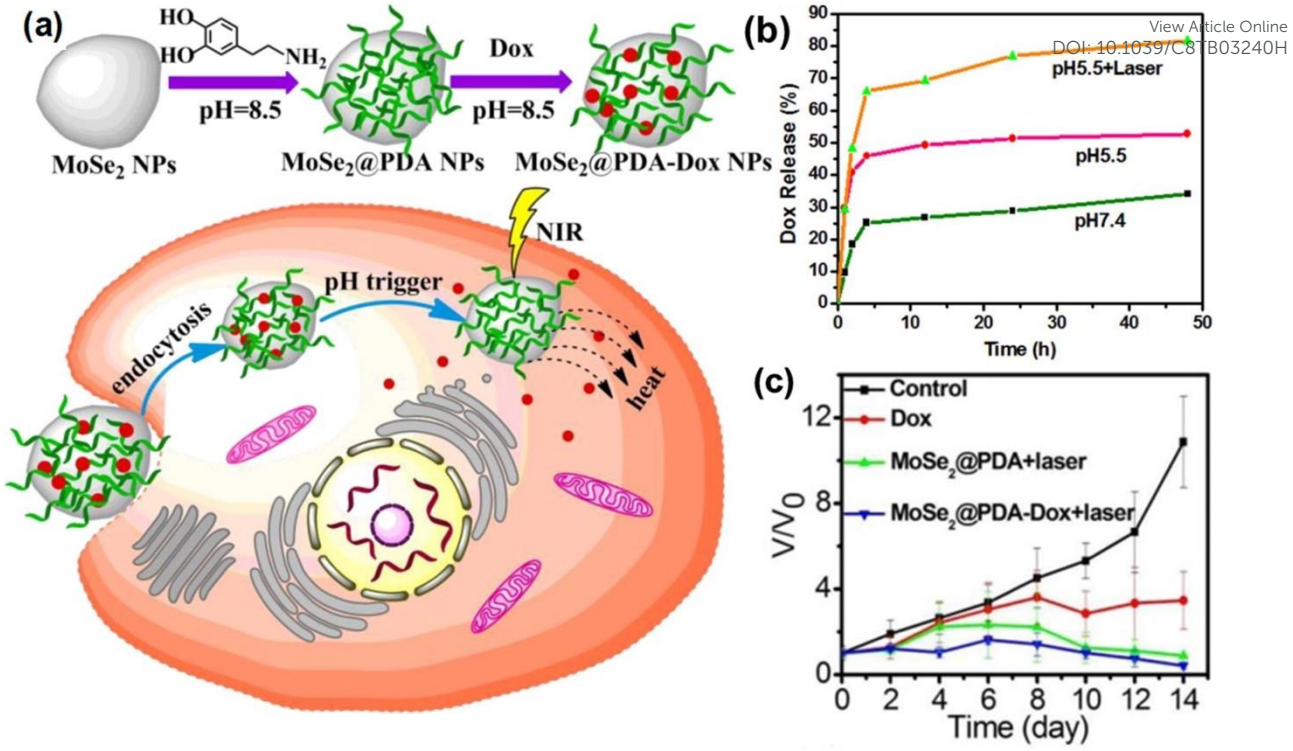

Fig.3 $MoSe_2$@PDA for pH- and heat-responsive drug release in chemo-photothermal synergistic therapy. (a) Schematic illustration of synthetic process and therapeutic mechanism of $MoSe_2$@PDA-DOX nanocomposites. (b) Release profiles of DOX from $MoSe_2$@PDA-DOX nanocomposites at pH 7.4, pH 5.5, and pH 5.5 with 808 nm laser irradiation. (c) Tumor growth curves of different groups after various treatment. The tumor volumes were normalized by comparison with their initial sizes. (Adapted from ref. 27, Copyright 2016, American Chemical Society. Reproduced with permission.)

maintaining and regulating cellular redox environment.[46,127] Therefore, the high intracellular GSH concentration in tumor cells presents opportunities to add GSH-sensitivity to light-responsive DDSs.[128] In this system, when MoS_2-PEI-PEG/DNA was trapped inside an endosome, laser irradiation could induce NIR-triggered endosomal escape. Afterward, DNA complex in the cytosol encountered the cellular redox environment, where GSH attenuated the disulfide bond, resulting in polymer detachment and DNA release. The sequential process initiated by exogenous and endogenous stimuli improved the efficiency of gene delivery and was promising to be applied for therapeutic applications.

NO is another therapeutic cargo which can be loaded on and released from the surface of TMDC nanomaterials under specific conditions. It has been confirmed that owing to its reducing power and byproducts dinitrogen trioxide (N_2O_3) and peroxynitrite ($ONOO^-$), NO plays a significant role in the natural immune system related to infection and then can cause lipid peroxidation, rupture of bacterial cell membranes and DNA deamination.[129,130] Most recently, NIR-mediated-releasing TMDC-based nano-carrier, MoS_2-BNN6, has been reported by Gao and co-workers for finely controllable bacteria-infected wound therapy.[131] In this system, *N,N*'-di-sec-butyl-*N,N*'-dinitroso-1,4-phenylenediamine (BNN6), as the NO donor, remained stable below 60 ℃, thus NO would not be released in physiological condition. Once irradiated by NIR light, MoS_2, with an excellent photothermal effect, could elevate the local temperature rapidly. Thus, with the temperature increasing to over 60 ℃, BNN6 would decompose to release NO and induce damage to DNA. Thus, by modulating NIR stimulus, NO could be used to kill cells in an on-demand manner without undesired release. In the experiment, the inactivation of bacteria of the group treated by MoS_2-BNN6 + NIR reached 98.9% for Amp^r *E. coli*, which was much higher than that of any other group. In addition, hyperthermia induced by MoS_2 could not only accelerate oxidation of GSH into GSSG, and disrupt the balance of antioxidants in the bacteria, but also induce PTT to cause the direct death of cells. Considering NO's good diffusion ability in tumor tissues, the PTT/NO synergetic strategy had a significantly enhanced effect on precise ablation of cancer cells upon NIR irradiation.[132-137]

Among the various TMDC-based NIR-responsive DDSs for cancer therapy, the most widespread use is to deliver chemotherapeutic drugs (*e.g.* doxorubicin (DOX) and 7-Ethyl-10-hydroxycamptothecin (SN38)) for specific chemotherapy. This system is able to overcome several shortcomings associated with chemotherapeutic drugs themselves, such as instability *in vivo*, short circulation period, poor water solubility and nonspecific delivery.[138,139] For a typical example, Yin *et al.* synthesized chitosan-functionalized MoS_2 (MoS_2-CS) NSs and loaded DOX onto it by physical absorbing.[107] NIR was used to trigger the on-demand drug release at tumor sites.[29] The release profile of DOX was examined and demonstrated that the accumulated release of DOX could approach 80% after being irradiated by 808 nm NIR laser with the power density of 1.4 W cm^{-2}, which was extremely higher compared to the DOX release in both MoS_2-CS-DOX group without NIR irradiation and the free DOX

group. As a result, the NIR laser light could be used as a stimulus to control the DOX release from MoS_2-CS-DOX system and thus enhanced the efficacy of tumor eradication.

To further enhance the therapeutic outcome, endogenous stimuli could also be introduced for the design of a more "smart" system for drug delivery. Among various endogenous "triggers", pH has been most widely used to design therapeutic platforms.[38] Due to the increased production and slow exportation of lactate and CO_2, the pH value in tumor sites is more acidic than that in blood and normal tissues.[140-142] Thus, combining pH and light stimuli in one platform seems an effective strategy for a more efficient tumor-targeting therapy.[6,114,143-145] For example, Wang *et al.* developed $MoSe_2$@PDA-DOX nanostructure and tried to combine the capability of pH-responsive drug release with PTT (Fig. 3).[27] The conjugated polydopamine (PDA) provided anchor points to load DOX onto the surface of $MoSe_2$ NSs by π-π stacking and hydrophobic interaction. At a mildly acidic environment, the interaction was attenuated and the release amount of DOX in PBS with pH 5.5 reached 50%, which was almost twice more than that at pH 7.4. Then, the release amount of DOX in the acidic environment kept increasing to 80% after 808 nm laser irradiation. Besides, PDA was also able to decrease the cytotoxicity and improve the photothermal effect of $MoSe_2$ NSs. According to an *in vivo* tumor model, the relative tumor volume change of the group of mice treated with $MoSe_2$@PDA-DOX + NIR was dramatically larger than that of the control group, and no tumor recurred during the following 15 days. As a result, such nano-system on the basis of $MoSe_2$@PDA-DOX nanocomposites could efficiently release drugs in response to pH and NIR light, and thus enhance the therapeutic effect.

In addition to 2D TMDCs, zero-dimensional (0D) TMDC nanodots (NDs) or quantum dots (QDs) with ultrasmall size could also be utilized in multi-stimuli-responsive platforms. The sizes of these nanoparticles are so small that they could escape the absorption of reticuloendothelial system, and be excreted through the kidney effectively rapidly, thus maximally avoiding the unwanted side effects.[34,89,91,100] As a representative example, a 0D TMDC nanoplatform based on WS_2 QDs (~5 nm) was synthesized by Lei and co-workers.[146] Upon reaching the mildly acidic TME, the tailored nano-medicine would quickly break into two segments, electropositive DOX@MSN-NH_2, and ultrasmall WS_2-HP. The former could be applied to kill surface tumor cells *via* chemotherapy, whereas the latter, with better biocompatibility and higher photothermal conversion efficiency, could penetrate the tumor parenchyma for NIR-induced PTT at deep tumor sites. Animal experiments showed that the group treated with both DOX@MSN-WS_2-HP and NIR laser light inhibited 93% of tumor growth. Thus, this multifunctional pH- and NIR-responsive nano-system could be introduced to conduct different therapeutic modalities for tumor cells at different tissue depths and accomplish programmed tumor therapy.

Most recently, to pursue a more "smart", controllable and highly efficient cancer treatment, two or more different endogenous stimuli have been integrated with TMDC-based light-responsive chemotherapeutic drug release. For instance, Zhang *et al.* synthesized copolymer and transferrin decorated MoS_2 NDs. Here, as shown in Fig. 4, the controlled drug release nanoplatforms could be responded simultaneously to both pH and GSH due to the Schiff base bond used to load DOX and the disulfide bond used to load thiol functionalized transferrin (Tf-SH).[33,147,148] For one thing, the two chemical bonds were pH-responsive. For another, the disulfide linkage was responsive to GSH, and it could be stable in the extracellular environment but could easily break down in the reductive intracellular compartment with a high GSH concentration. The maximum release of DOX was 69.3% under tumor acidic pH conditions (pH = 5.7) with a high GSH concentration (10 mmol L^{-1}) after 48 h. Along with NIR irradiation, this study demonstrated a multi-model and renal-clearable theranostic system for chemo-photothermal therapy based on smart nano-carriers. In another work conducted by Dong and co-workers, they reported an intelligent nanoplatform on the basis of DOX-loaded MoS_2-PEI-HA NSs for targeted and enzyme-/pH-/NIR-responsive drug delivery.[149] On the one hand, HA can not only combine with a CD44 receptor, targeting CD44-overexpressing breast cancer (MCF-7-ADR), but also be degraded by HAase, one of the most closely cancer-related enzyme, thus accelerating DOX release from MoS_2 based NSs. On the other hand, the mildly acidic TME and external NIR laser irradiation could promote the DOX release. Thus, the drug release was controlled and accelerated by the three parts, leading to more precise elimination of cancer cells. It was found that the maximum cumulative release ratio of DOX, up to 77.4%, was from the group with all the three parts, HAase (0.5 mg mL^{-1}), NIR laser irradiation (808 nm, 0.6 W cm^{-2}) and acidic condition (pH = 5.0). Furthermore, this platform was also confirmed to overcome chemotherapy resistance, because the combination of HA targeting and mild NIR laser stimuli was capable of downregulating the expression of drug-resistance-related P-glycoprotein (P-gp). Therefore, it could reverse drug resistance and enhance intracellular drug accumulation so as to significantly improve therapeutic outcomes in drug-resistant cancer.

4. Stimuli-responsive platform based on TMDC for deep cancer therapy

Although NIR laser has been widely used as a trigger for TMDC-based cancer therapy and several successful experiments proved the good performance of NIR laser, the penetration of NIR light is limited (1–3 mm)[150], so that it can only be used to kill the malignant tissues on the surface of the body. However, tumors are mostly located inside the body. Thus, it is desirable to develop a kind of treatments with no penetration restriction. For this purpose, magnetic field, X-ray, and microwave are more preferable, since these stimuli demonstrate better penetrating efficacy for deep-sited cancer therapy.[45]

4.1 Magnetic field-responsive platform based on TMDC for deep cancer therapy

Magnetism has been widely applied for diagnosis and therapy of cancer since it almost has no harm on the body and possesses high tissue penetration ability. MRI, a conventional imaging approach, was developed in the early 1970s. It involves the detection of nuclear spin reorientation in the external magnetic field. Compared

View Article Online
DOI: 10.1039/C8TB03240H

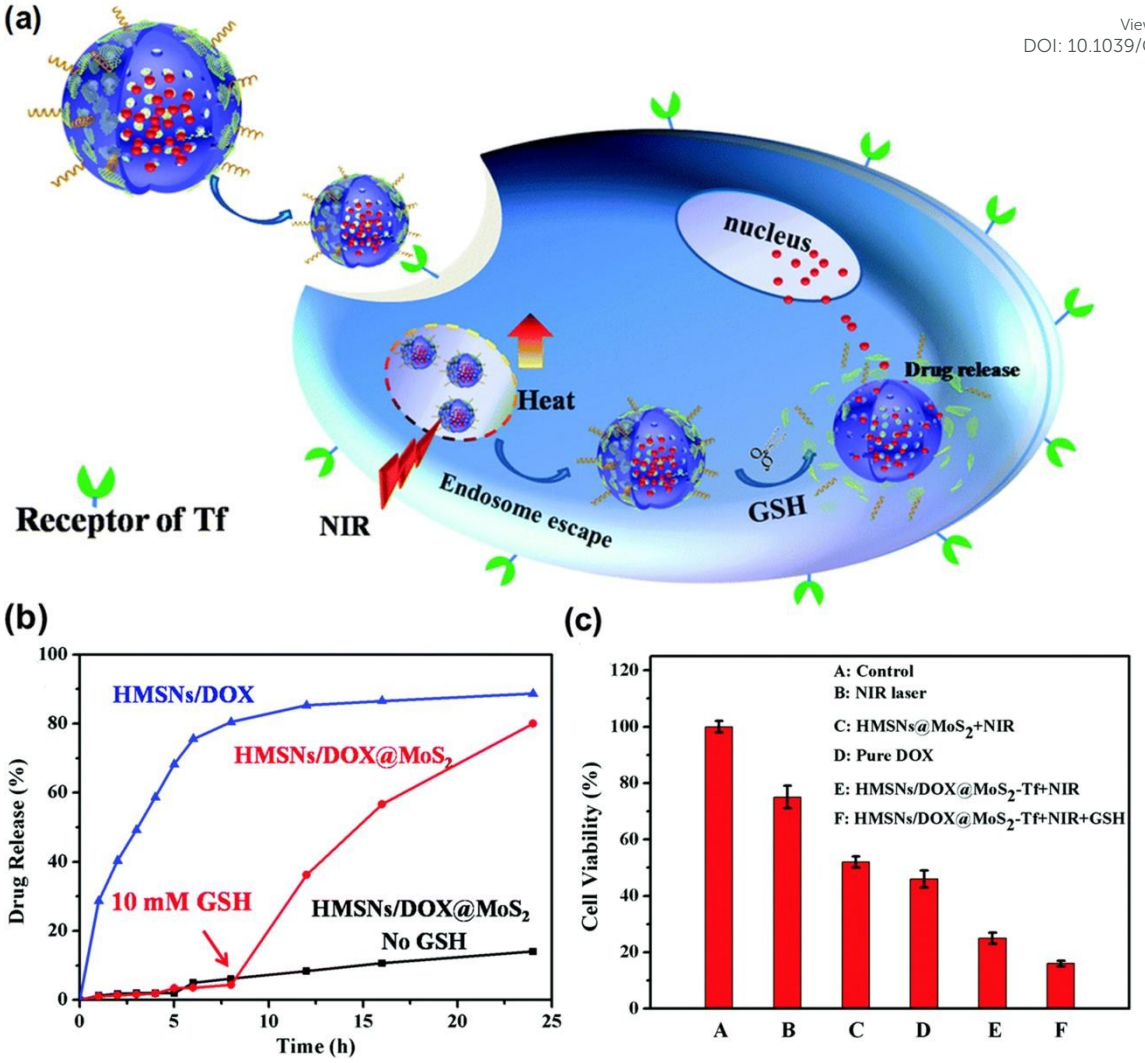

Fig.4 Transferrin-decorated, MoS_2-capped hollow mesoporous silica nanospheres (HMSNs/DOX@MoS_2-Tf) as a targeting chemo–photothermal synergetic system controlled by both NIR and GSH. (a) Schematic illustration of targeted drug delivery, photothermal therapy and GSH-triggered drug release with HMSN/DOX@MoS_2/Tf nanocomposites. (b) Drug release profile of HMSNs/DOX, HMSNs/DOX@MoS_2 and the stimuli-triggered DOX release profile for HMSNs/DOX@MoS_2 upon the addition of 10 mM GSH. (c) Cell viabilities of HeLa cells treated with NIR laser, pure DOX, HMSNs@MoS_2 with NIR, HMSNs/DOX@MoS_2-Tf with NIR laser and HMSNs/DOX@MoS_2-Tf with NIR laser as well as GSH. (Adapted from ref. 148, Copyright 2017, The Royal Society of Chemistry. Reproduced with permission.)

to X-ray CT, which is suitable to provide images of tissue anatomy, MRI is more suitable for molecular imaging of tissue function.[75,151,152] To further increase the sensitivity and avoid the effect of water in the biological body, many contrast agents containing magnetic metal ions have been used in MRI scans.[75,153,154] Contrast-enhanced MRI is one of the most reliable and non-invasive diagnostic methods because it can provide an assessment of disease pathogenesis, timely feedback information about disease tissue, and high-resolution 3D anatomical images of soft tissues.[155-158] Therefore, guided by bioimaging, cancer therapy could be more pointed and precise, leading to an enhanced therapeutic effect.

Gd(III) chelate is one of the most widely used contrast agents due to its distinctive electronic structure.[153,159] For example, Chen and co-workers tried to design BSA-Gd-complex-modified MoS_2 nanoflakes as cancer theranostic agents for MR/PA imaging and PTT.[95] The PTT efficacy was investigated on the 4T1-bearing mice model and demonstrated that compared to other groups, tumors treated with MoS_2-Gd-BSA and NIR laser were dramatically inhibited without regrowth in the next 2 weeks. Furthermore, to guarantee the precision of PTT, some imaging tools would be used for assistance. On the one hand, the outstanding photothermal performance enabled the MoS_2-Gd-BSA nanomaterials as promising photoacoustic contrast agents. On the other hand, the T_1-weighted MR images were increasingly brighter with the increasing concentration of Gd. The transverse relaxivity r_1 was calculated and showed that the r_1 value of MoS_2-Gd-BSA was 17.95 $mmol^{-1}$ s^{-1} L, 4 times higher than that of the commercial Gd-diethylenetriaminepentaacetic acid (DTPA). Thus, it showed that the images of MoS_2-Gd-BSA were much brighter than those of Gd-DTPA with the same concentration of Gd, indicating that the as-synthesized MoS_2-Gd-BSA had great potential for cancer

View Article Online
DOI: 10.1039/C8TB03240H

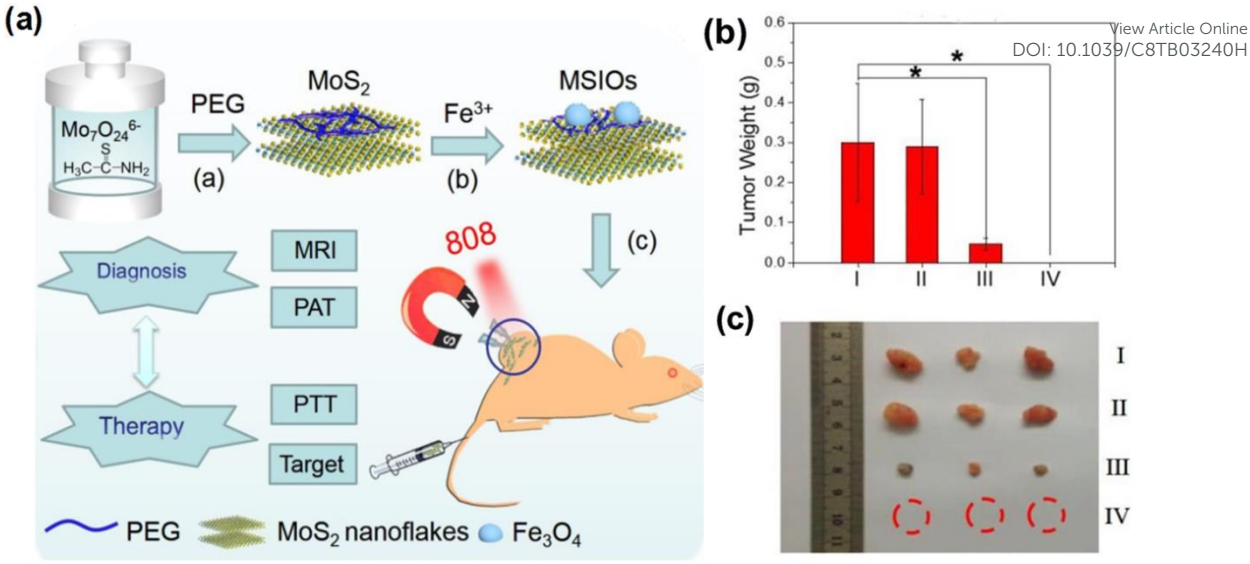

Fig.5 MoS_2/Fe_3O_4 nanotheranostic for magnetically targeted photothermal therapy. (a) Schematic illustration of the synthesis route and theranostic procedure of MSIOs for dual-modal MR and PAT imaging-guided magnetic targeting photothermal ablation of cancer. (b,c) *In vivo* magnetic targeting-enhanced cancer therapy. Four groups of tumor-bearing mice with subcutaneous tumors were used: (I) PBS injection, (II) PBS +NIR laser exposure, (III) MSIOs + NIR laser, and (IV) MSIOs + magnetic targeting + NIR laser. (b) Tumor weights after the treatment of 15 days. P values: *p < 0.05. (c) Representative photos of tumors in the four groups after treatment of 15 days, suggesting an effective treatment for the magnet targeting PTT *in vivo*. (Adapted from ref. 161, Copyright 2015, Ivyspring International Publisher. Reproduced with permission.)

theranostics.

Apart from the magnetic property of Gd(III), some of the TMDC materials themselves could be used as MRI contrast agents. Chen *et al.*, for the first time, presented VS_2@lipid-PEG nanoparticles to enhance *in vivo* MR imaging and thus realize multi-modal imaging-guided photothermal tumor ablation.[160] Apart from the high NIR absorbance and photothermal conversion efficiency of VS_2, since vanadium (V) has $3d^1$ electronic configuration and strong electron coupling, VS_2 processes a new class of paramagnetic properties. The brightness of T_1-weighted MR images was progressively improved with the increasing concentration of V. *In vivo* MR imaging also showed an obvious brightening effect in T_1-weighted MR signals in the tumor of mice after 24 h injection of VS_2@lipid-PEG. With strong NIR absorbance and chelator-free radiolabelling ability, the VS_2@lipid-PEG nanoparticles could also act as photoacoustic and single photon emission computed tomography imaging. Thus, the obtained nanomaterials based on VS_2 could be developed for a tri-modal imaging-guided therapeutic platform and further enhance the effect of PTT and may be a promising type of nanomaterials for theranostic applications.

Magnetic stimulus can be used for magnetically targeted cancer therapy as well. The work conducted by Yu and co-workers is a representative example (Fig. 5).[161] They integrated MoS_2 flakes with Fe_3O_4 nanoparticles (MSIOs) and functionalized it with biocompatible PEG. The anchoring strength between Fe_3O_4 nanoparticles and MoS_2 nanoflakes was not only because the large surface area of MoS_2 offered more chances to absorb the Fe_3O_4 nanoparticles, but also due to its negative charged surface which, through electrostatic interaction, could be anchored with positive-charged Fe^{3+} more easily. Thus, Fe_3O_4 nanoparticles could be loaded on MoS_2 nanoflakes in a controllable way by varying the concentration of Fe precursor. Then directed by external magnetic field, Fe_3O_4 on the surface of the nanomaterial could serve as target moiety, enhancing the accuracy of PTT. The magnetic targeting induced therapeutic effects were evaluated both in Hela cells and in tumor-bearing mice. In *in vitro* experiment, the cells in the experimental group were cultured with MSIOs (10 μg mL^{-1}) with a donut-shaped magnet beneath the culture plate. It has been observed that under NIR laser irradiation, quantities of cells surrounding the magnet were destroyed and especially, those in the center of magnetic field were almost absolutely eliminated. Compared with the high cell viability in the control group, the as-prepared materials exhibited remarkable magnetic targeted enhanced PTT properties. In addition, animal experiment showed that tumor volume in the group injected with MSIOs (100 μL, 1 mg mL^{-1}), irradiated with NIR laser (808 nm, 0.6 W cm^{-2}) and applied with external magnetic field began to decrease after 2 days. After 9-day treatment, these tumors almost disappeared with no recurrence during the next 15 days. Compared to the slight changes in other groups, it exhibited the best treatment effect. Thus, such multifunctional PEG-modified MoS_2/Fe_3O_4 nanocomposites can be utilized for magnetic targeted drug release, imaging (MRI), along with hyperthermal therapy.

4.2 X-ray-responsive platform based on TMDC for deep cancer therapy

X-ray is another external stimulus which has been most widely used for CT and RT.[162,163] The most important advantage is that due to the better penetration of X-ray, it can be precisely controlled to eliminate deep-sited tumor cells, and the treatment can be restricted to a specific body part, including breast, lung, and brain

View Article Online
DOI: 10.1039/C8TB03240H

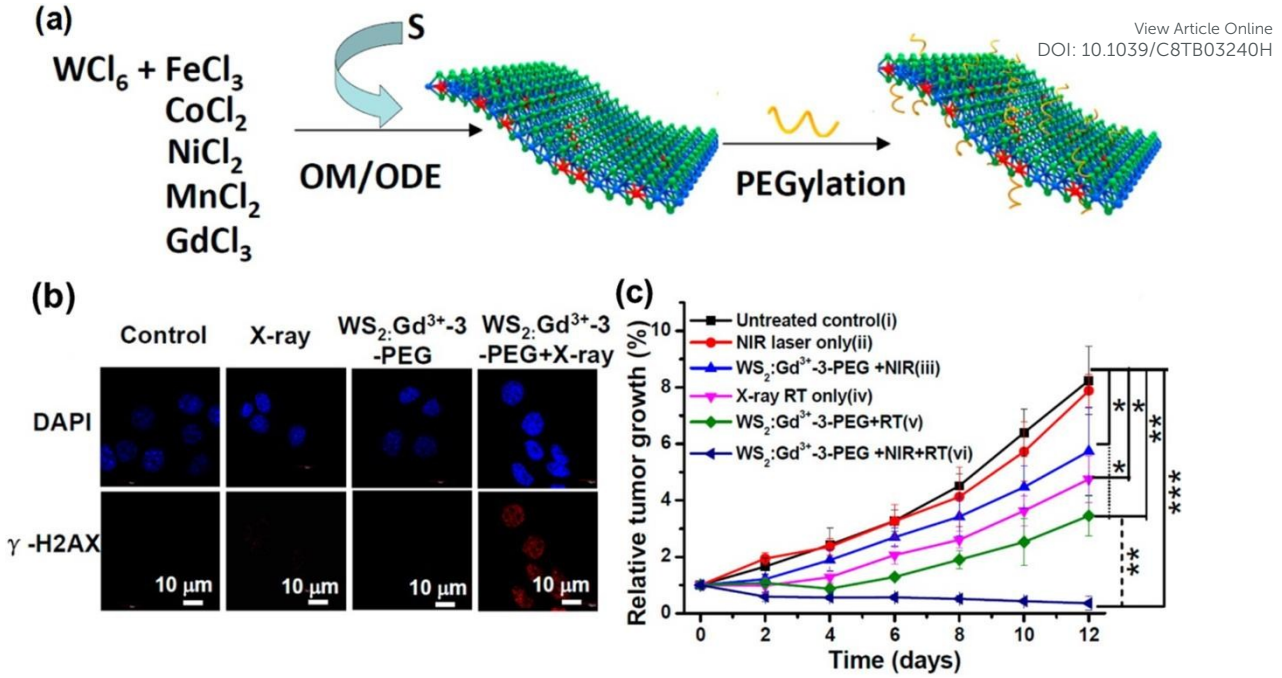

Fig.6 WS_2: M^{n+} (M = Fe^{3+}, Co^{2+}, Ni^{2+}, Mn^{2+}, and Gd^{3+}) nanoflakes for multimodality tumor imaging and combined PTT/RT. (a) Schematic illustration of the one-pot synthesis of metal-ion-doped WS_2 nanoflakes and the subsequent surface modification with PEG. (b) *In vitro* photothermal therapy and radiation therapy: Confocal fluorescence images of γ-H2AX-stained 4T1 cells treated with PBS control, RT alone (4 Gy), WS_2: Gd^{3+}-3-PEG control, and WS_2: Gd^{3+}-3-PEG + RT (4 Gy). (c) *In vivo* combined photothermal and radiation therapy: Tumor volume growth curves of mice after various treatments (5 mice for each group). Group i: untreated control; group ii: NIR laser only; group iii: WS_2: Gd^{3+}-3-PEG + NIR; group iv: X-ray RT alone; group v: WS_2: Gd^{3+}-3-PEG + RT; group vi: WS_2: Gd^{3+}-3-PEG + NIR + RT.PTT was conducted by the 808 nm laser at 0.5 W cm^{-2} for 10 min, while the irradiation dose of RT was 4 Gy. Error bars were based on standard error of the mean (SEM). Statistical analysis was performed using the Student's two-tailed t test: *$p < 0.05$ and **$p < 0.01$. (Adapted from ref. 167, Copyright 2015, American Chemical Society. Reproduced with permission.)

tumors.[164] However, the radio-resistance of solid tumors, especially tumor hypoxia, limits the efficiency of RT. One of the strategies utilized to overcome the drawback of RT is to apply radiosensitizers, which can accelerate DNA damage, produce free radicals, and eventually enhance injury to tumor tissues. Furthermore, mild PTT heating could also improve oxygenation status and help to overcome the hypoxia-associated resistance of tumors to X-ray radiation (Fig. 6).[165-167] Thus, certain types of TMDC nanomaterials with high-*Z* elements and salient photothermal effects, could efficiently serve as radiosensitizers and be applied for tumor theranostics in RT and the combination with other therapy.[85,165,166,168,169]

For example, Wang *et al.* synthesized MoS_2/Bi_2S_3-PEG (MBP) composite NSs to take advantage of both MoS_2 and Bi_2S_3 for combined photothermal- and radio- cancer therapy.[170] Bismuth (Bi)-containing composites possess a strong photoelectric absorbance capacity under X-ray radiation, which can be applied to improve the X-ray deposition within tumor tissue and accelerate the break in DNA. In addition, MoS_2, with high absorption in NIR irradiation, could assist PTT and PA imaging. Therefore, such an MBP composite nano-system performed well both *in vitro* and *in vivo* CT/PA imaging-guided tumor diagnosis and combined PTT and RT treatment. Firstly, the HU values of tumors were dramatically increased after injection of MBP NSs *via* both i.v. and i.t. route into 4T1 tumor-bearing mice, indicating the advantage of using such materials in precise CT imaging of tumors. Secondly, in animal experiment, the PA signal intensity of tumors after administration of MBP NSs was 1.5 times stronger than that of the control group, demonstrating the positive effect on PA imaging. Finally, after X-ray irradiation, compared to tumors in MP-treated mice, more vacuoles, condensed nuclei, and changed cell shapes were found in the MBP-treated mice, showing a better anticancer effect. Furthermore, it was found that after successive exposure to 808 nm laser (0.8 W cm^{-2}, 5 min) and X-ray irradiation (8 Gy), MBP-treated ([Mo] = 100 ppm, 30 μL), mice experienced a dramatically suppressed tumor growth without recurrence. Thus, 2D MBP NSs showed great promise in imaging-guided tumor diagnosis and such combination of PTT/RT could realize an enhanced tumor growth inhibition.

Apart from the improvement of EBRT, TMDC with a high-*Z* element could also be applied to enhance the efficiency of IRT. In the work conducted by Chao *et al.*, rhenium-188 labelled tungsten disulfide (WS_2) nanoflakes were synthesized.[166] In this nano-system, ^{188}Re, as a radioisotope, could emit radioactive γ-radiation, while tungsten (W) was used to absorb ionization radiation generated from ^{188}Re, enabling "self-sensitization" to enhance the efficacy of RIT. Meanwhile, WS_2-PEG, with strong NIR absorbance, could be used for NIR light-induced PTT, which could enhance the RIT efficiency at the same time. Therefore, after i.t. injection of ^{188}Re-WS_2-PEG, self-sensitized and NIR-enhanced RIT would be realized, completely ablating cancer cells. The results clearly showed that for mice treated with both NIR-enhanced RIT and

View Article Online
DOI: 10.1039/C8TB03240H

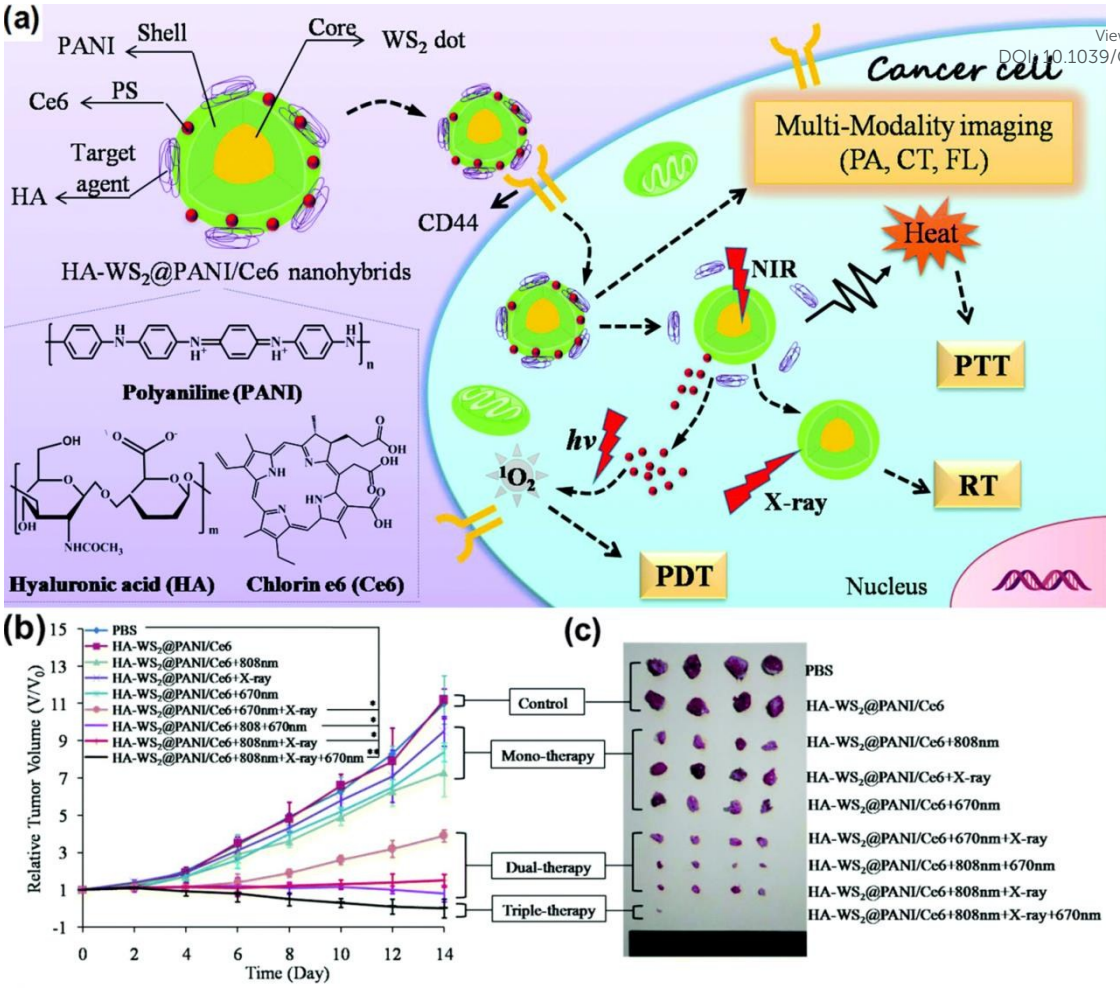

Fig.7 A triple-synergistic nanoplatform for combinational RT/PTT/PDT and multi-modality imaging based on HA-WS_2@PANI/Ce6. (a) Schematic illustration of HA-WS_2@PANI/Ce6 nanohybrids for the multi-modality imaging-guided tri-model combination therapy of tumors. (b) Growth of 4T1 tumors in different groups of mice after treatment. The relative tumor volumes were normalized to their initial sizes. *P < 0.05, **P < 0.01. (c) Photos of tumors collected from each group of the 4T1 tumor-bearing mice after various treatments. (Adapted from ref. 165, Copyright 2017, The Royal Society of Chemistry. Reproduced with permission.)

^{188}Re-WS_2-PEG, their tumors were eradicated and all of the mice remained healthy over two months. Compared to the well therapeutic effects, the untreated mice or free ^{188}Re-treated mice only survived for 16–20 days, and for mice treated with only RIT plus ^{188}Re-WS_2-PEG or only PTT plus WS_2-PEG, their life-spans just lengthened to 22–30 days. Thus, due to the radioisotopes delivery into tumors, this work enabled "self-sensitization" to induce cell damage, modulated the hypoxia state of tumors, and successfully enhanced the therapeutic efficacy.

Recently, TMDCs, which are able to work as both photothermal agents and radiosensitizers, are becoming popular because of their multifunctional properties and simple synthetic methods. Yong *et al.* fabricated 3 nm-WS_2 QDs with excellent NIR absorbance and X-ray attenuation property for PTT/RT synergistic treatments.[34] The results showed thorough tumor elimination 5 days after being treated with WS_2 QDs + PTT + RT without re-growth in 17 days, which is the most efficient tumor growth delay compared with PTT or RT alone. It demonstrated that the as-prepared WS_2 QDs could convert NIR laser irradiation into heat and increasing the temperature of the tumor tissues to ~45 ℃. Then the NIR-mediated mild temperature elevation could change the oxygenation environment to enhance the therapeutic effects of RT. Therefore the newly-synthesized nanocomposites could realize a synergistic PTT/RT without causing long-term toxicity *in vivo*.

For further enhanced therapeutic effects, Wang and co-workerstried to introduce PDT and develop a nanoplatform (HA-WS_2@PANI/Ce6) to realize targeted triple-therapy (PDT/PTT/RT) (Fig. 7).[165] In this system, irradiated by 808 nm NIR laser, HA-WS_2@PANI/Ce6 served as an efficient photothermal agent for targeted PTT. Then the hyperthermia caused by PTT could result in the acceleration of blood flow and the increase of oxygen supply in the tumor. Sufficient oxygen, could not only improve the PDT efficiency due to the increase in the production of $^1O_2$, but also enhance the RT effect by reducing the radioresistance of the tumor. In animal experiment, the relative tumor volume change of the triple-therapy group indicated that the tumor growth was completely inhibited without recurrence in the observation period, while fast tumor growth and tumor recurrence were obtained in

View Article Online
DOI: 10.1039/C8TB03240H

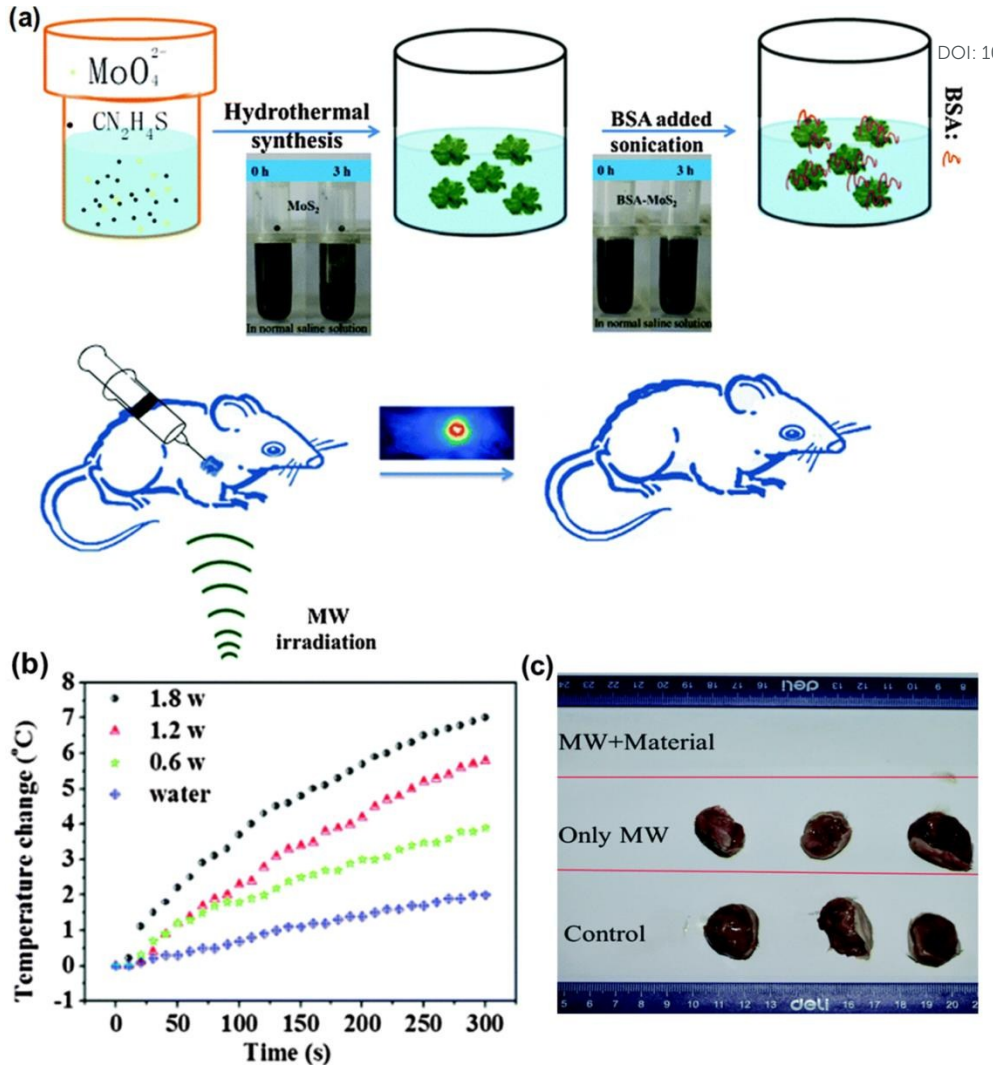

Fig.8 Layered MoS_2 nanoflowers for microwave-responsive thermal therapy. (a) Schematic illustration of the synthesis process of BSA-MoS_2 nanoflowers as nanoagents for efficient cancer MW thermal therapy. (b) MW heating of BSA-MoS_2 dispersed in deionized water at different power (0.6 W, 1.2 W and 1.8 W). (c) Photos of collected tumors of each group. (Adapted from ref. 180, Copyright 2016, The Royal Society of Chemistry. Reproduced with permission.)

the single- and dual-therapy group, respectively. Thus, this novel TMDC-based nanoplatform could overcome the tumor resistance of hypoxia-related RT/PDT and display a highly enhanced strategy for cancer therapy.

4.3. Microwave-responsive platform based on TMDC for deep cancer therapy

Compared to the side effect caused by chemotherapy and RT, thermal therapy is a relatively non-invasive, simple approach to treat tumors. It converts NIR laser[171-173] or MW irradiation into heat and then hyperthermia can kill the cells through protein denaturation or rupture of the cellular membrane, leading to the removal of cancerous cells and the shrink of tumor.[174] Since NIR light has a limited penetration depth, typically 1–3 mm, thermal therapy induced by NIR laser cannot reach underlying tumors to treat large tumors. Whereas, MW shows a longer penetration depth, faster heat generation, shorter irradiation durations, large ablation zones and less susceptibility to local heat sinks.[86] However, simple heating techniques have difficulty discriminating between tumors and surrounding healthy tissues, leading to serious damage to normal tissues and unbearable pain. In order to facilitate localized heating and enhance the efficiency for cancer treatment, MW susceptible agents with spatial confinement microcapsule walls, such as TMDC nanomaterials, have been widely investigated and then applied in clinical cancer treatments. Taken layered MoS_2 NSs as an example, the dipolar polarization and ionic conduction of layered MoS_2 NSs are the two main causes of the heating effect of MW.[175] Irradiated by MW, the dipoles or ions would align in the oscillating electric field. Then the molecular friction and dielectric loss would generate heat, which could dramatically change the states of the molecules or ions in nanoscale spaces, and further improve the effect of heating.[176-179] Wang *et al.*, for the first time, applied layered MoS_2 nanoflowers, as MW susceptible agents for

MW thermal therapy (Fig. 8).[180] After 5-min MW irradiation, the temperature of BSA-MoS_2 dispersed in normal saline increased by 25 ℃, while the temperature of NSs and water could only increase by 14 ℃ and 2 ℃, respectively. Therefore, the BSA-MoS_2 dispersed in saline solution showed enhanced MW thermal effects, demonstrating that the as-prepared MoS_2 nanomaterials had outstanding MW susceptible properties. In *in vivo* experiment, contrast to the quick growth for the control group and only MW group, tumor growth was completely inhibited for the material+ MW group. After 17 days, tumors for the material + MW group disappeared and no apparent change in tissues was detected. Therefore, BSA-MoS_2 turns out to be a promising susceptible agent for cancer therapy *via* MW ablation.

Though many novel MW susceptible agents were introduced to treat tumors, to realize complete ablation of the large orthotopic transplantation tumor or tumor cells remained in the periphery is still difficult. In order to overcome the heat-sink effect induced by the blood flow and other difficulties,[181] Fu and co-workers encapsulated MoS_2 NSs in sodium alginate microcapsules (MSMCs) as MW embolization agents for large orthotopic transplantation tumor therapy.[182] According to the results of the *in vivo* MW therapy on mice, the temperature of the tumor region receiving MSMC immediately increased to 50 ℃ after mere 1-min MW irradiation and reached 60 ℃ in 5 min. The hyperthermia was so high and persistent that it could realize a complete ablation of the cancer cells and prevent their re-growth. It was found that the tumor suppression rate in the group of MW, MC + MW, MoS_2 NSs + MW, and MSMC + MW group was 59%, 69%, 79%, and 100%, respectively, indicating an effective tumor ablation of MSMC. Furthermore, the ablation region of the group receiving MSMC + MW was 5 times larger than that of the group treated by MW alone. Considering the good biocompatibility and clearance from the body, MSMC could potentially be applied as a multifunctional theranostic agent for treatment of the larger tumor *via* the synergistic therapy of enhanced MW ablation and transcatheter arterial embolization.

5. Conclusions and Outlooks

In this review, we summarize the recent advances in TMDC-based stimuli-responsive mechanisms and applications to cancer treatment. Compared with other nanomaterials, 2D TMDCs have some special characteristics, making them novel and promising biomedical platforms. However, TMDCs are relatively new, and many drawbacks remain. The details about the current problems, subsequent developments and future directions are discussed in the following part.

First of all, biosafety should be paid more attention to in biomedical applications. Though compared to other typical materials, TMDCs induce fewer cytotoxic responses and are more biocompatible, several problems still need to be considered. On the one hand, the *in vivo* biodistribution, metabolic pathways, and excretion of TMDCs are important in practical use. Some inert inorganic nanomaterials end up accumulating in the living body, bringing long-term toxicity and side effects.[17] On the other hand, some compounds that are conjugated or coated with TMDCs, such as Fe_3O_4, are not biodegradable.[45] The degradation of these materials can release metal ions and cause negative effects on living organisms for a long time.[45] So far, one of the most accepted strategies is to reduce the particle sizes to ensure easy excretion, complete clearance, and enhanced biosafety. For example, instead of 2D TMDCs, some researchers fixed their attention on 0D TMDC NDs or QDs with ultrasmall sizes, which successfully demonstrated efficient tumor inhibition and improved biocompatibility.[34,89,91] Before final clinical translation, more efforts are still required on the study of the material toxicity.

Secondly, synthetic methods and surface functionalization strategies should be optimized. Though many physical and chemical preparation approaches have been provided, such as liquid exfoliation method and electrochemical intercalation methods,[183-185] most of them still lack better control on the thickness and size of the products. Therefore, the therapeutic effect of these materials will significantly decrease. Considering that the complexity of TMDC architectural design and difficulties scaling up the synthesis may restrict their further applications, not only the industrial-scale and controllable production, but also the efficiency repeatability of synthesis and functionalization require to be realized and further improved in the near future.[1,29]

Thirdly, the long-term stability and durability under stimulus is also important and needed to be improved. The internal (*e.g.* acidity, GSH, specific enzyme overexpression, and ATP) and the external signals (*e.g.* light, MW, and radiation) may have negative effects on the long-term stability of TMDC. Though the instability may stimulate the degradation of materials to reduce the inherent toxicity, it causes more problems. For example, it may bring about side effects and weaken, even deprive the therapeutic effects of the responsive nano-system. Thus, the TMDC-based stimuli-responsive system may only work for a short period with a worse therapeutic result. Since the previous research did not pay enough attention on this issue, more experiments should be conducted to fix this problem.[8]

Additionally, standard of evaluation criteria for the stimuli-responsive therapeutic platforms is still a challenging aspect in this field.[29] According to the research mentioned above, these smart platforms all have their own advantages, but it is difficult to pinpoint which stimuli-responsive nano-system provides the best treatment and causes the least side effects. Considering the general rule, the simpler and easier the development of a system is, the better its chances of reaching the clinic. Multi-stimuli-responsive systems may have some advantages compared to the simple ones. However, the contribution of each stimulus and the principle of multiple stimuli working together to enhance the effect are still not clear. Besides, multi-stimuli-responsive systems are more difficult to be constructed. Thus, establishing reasonable evaluation criteria to measure the chances of clinical applications is instrumental for the future development.[1]

Last but not least, the overall therapeutic efficacy of TMDCs remains in a low stage. Each therapeutic modality has its own limitations. For example, light-responsive therapies (*e.g.* PTT, PDT) cannot penetrate deep enough to kill deep-sited tumors, while pH-triggered therapies have much lower flexibility.[142] Also, to ensure the accuracy of treatment, imaging guidance could be

View Article Online
DOI: 10.1039/C8TB03240H

Table 1 Overview of TMDC-based materials applied in stimuli-responsive systems.

Materials	Cancer Types	Active Moiety	Synthetic Method	Stimulus	Therapeutic Types	Ref.
MoS_2	MDA-MB-468 cells, MCF-7 cells	aptamer, DOX, DNA	Liquid-phase exfoliation method	ATP	Chemotherapy, ATP targeted delivery	186
	HeLa cells	thiolated DOX, 6-mercaptopurine	Liquid exfoliation and solvothermal method	GSH	Chemotherapy, GSH targeted delivery	128
	HeLa cells	/	Morrison method	NIR	PTT	105
	4T1 cells	generation 5 (G5) poly-(amidoamine) dendrimers- LA, B-cell lymphoma-2 siRNA	Hydrothermal method	NIR	PTT + GT	187
	HepG2 cells	BSA, Cy5.5	Hydrothermal method	NIR	PTT + PDT, PA/FL imaging	188
	4T1 cells	PEG, Ce6, AuNPs	Liquid exfoliation method	660 nm and 808 nm light, X-ray	PTT + PDT, CT/NIRF imaging	189
	4T1 cells	PEG, IONPs, ^{64}Cu	Morrison method	NIR, magnetic field	PTT, PA/MR/PET imaging	13
	Panc-1 cells	PEG, IONPs	Hydrothermal method	NIR, magnetic field	PTT, MR/PA imaging, magnetic field targeted delivery	161
	SCC-7 cells, COS-7 cells	LA-PEG, LA-K_{11}(DMA), toluidine blue O	Ultrasonic exfoliation method	NIR, pH	PTT + PDT, pH targeted delivery	115
	HeLa cells	DOX, transferrin, hollow mesoporous silica NPs	Solvothermal method	NIR, GSH	PTT + Chemotherapy	148
	HCT116 cells, B16F1 cells	PEG, thiolated PEG, LA-PEI, DNA	Chemical exfoliation method	NIR, GSH	GT, CT imaging, GSH targeted delivery	126
	4T1 cells, KB cells, HeLa cells	DOX, LA-PEG-FA	Morrison method	NIR, FA receptor	PTT + Chemotherapy	144
	HeLa cells	aptamer, Ce6	Liquid exfoliation method	NIR, ATP	PDT, ATP targeted delivery	190
	A549 cells	aptamer, DOX, PEG, $Cu_{12}S$	Ultrasonic exfoliation method	NIR, microRNA	PTT + Chemotherapy, PL/PT imaging, miRNA targeted delivery	191
	4T1 cells	CS, AlPc, SiO_2	Liquid exfoliation method	NIR, pH, X-ray	PTT + PDT + Chemotherapy, PA/CT/NIRF imaging, pH targeted delivery	114
	LO2 cells, Hep3B cells	CS, Fe_3O_4, Mn, metformin	Solvothermal method	NIR, pH, magnetic field	PTT + Chemotherapy, MR imaging, pH targeted delivery	192
	HepG2 cells	DOX, POV, thiolated transferrin	Hydrothermal method	NIR, pH, GSH	PTT + Chemotherapy, pH/GSH targeted delivery	147
	MCF-7-ADR cells	DOX, PEI, HA	Liquid-phase exfoliation method	NIR, pH, enzyme	PTT + Chemotherapy, PET imaging, pH/enzyme targeted delivery	149
	VX-2 liver orthotopic transplantation tumor	DOX, mPEG-PLGA, Fe_3O_4	Hydrothermal method	MW, X-ray, magnetic field	MW thermal therapy, CT/MR imaging	181
MoS_2/Bi_2S_3	HT29 cells	DOX, PEG, agar	Solvothermal method	NIR, pH, X-ray	PTT + Chemotherapy, CT/PA imaging, pH targeted delivery	193
	4T1 cells	PEG	Solvothermal method	NIR, X-ray	PTT + RT, CT/PA imaging	170
WS_2	4T1 cells	LA-PEG	Morrison method	NIR	PTT	106
	HCT-116 cells	DOX, PMOs	Solvent exfoliation method	NIR	PTT + Chemotherapy	100
	4T1 cells	DOX, MSN	Grinding and sonication method	NIR, pH	PTT + Chemotherapy, pH targeted delivery	146
	HT29 cells	PVP	Hydrothermal method	NIR, X-ray	PTT, CT/PA imaging	194
	BEL-7402 cells	PEI, siRNA	Liquid exfoliation method	NIR, X-ray	PTT + GT, CT/PA imaging	123
	HeLa cells	BSA, methylene blue	Liquid-phase exfoliation method	665 nm and 808 nm light, X-ray	PTT + PDT, CT imaging	104

View Article Online
DOI: 10.1039/C8TB03240H

Materials	Cancer Types	Active Moiety	Synthetic Method	Stimulus	Therapeutic Types	Ref.
	4T1 cells	Ce6, HA, PANI	Solvothermal method	670 nm and 808 nm light, X-ray	PTT + PDT + RT, CT/PA/FL imaging	165
	4T1 cells	PEG, Gd^{3+}	Solution-phase method	NIR, X-ray, magnetic field	PTT + RT, CT/PA/MR imaging	167
	4T1 cells	DOX, PEG, Fe_3O_4 NPs, mesoporous silica, Cy5.5	Lithium intercalation method	NIR, pH, X-ray, magnetic field	PTT + Chemotherapy, CT/MR imaging, pH targeted delivery	102
	4T1 cells	PEG, ^{188}Re	Hydrothermal method	NIR, X-ray	PTT + RIT	166
ReS_2	4T1 cells	PEG, $^{99m}Tc^{4+}$	Hydrothermal method	NIR, X-ray	PTT + RT, CT/PA imaging	168
	HeLa cells, Panc-1 cells	PVP	Liquid exfoliation method	NIR, X-ray	PTT, CT/PA imaging	195
TaS_2	HeLa cells, PC3 cells	DOX, 1,2-distearoyl-sn-glycero-3-phosphoethanolamine-N-[methoxy(PEG)-3000]	Grinding and sonication method	NIR, pH, X-ray	PTT + Chemotherapy, CT imaging, pH targeted delivery	196
TiS_2	4T1 cells	PEG	Solution-phase method	NIR	PTT, PA imaging	94
VS_2	4T1 cells	PEG-lipid, $^{99m}Tc^{4+}$	Ultrasonic exfoliation method	NIR, magnetic field	PTT, PA/MR/PET imaging	160
	HeLa cells	DOX, PVP	PVP-assisted exfoliation method	NIR	PTT + Chemotherapy	197
	4T1 cells	indocyanine green	Solution-phase method	NIR	PTT, PA imaging	198
	SPC-A-1 cells	PLGA, FA, PEG-lipid	Liquid exfoliation method	NIR, FA receptor	PTT	199
$MoSe_2$	HepG2 cells, 3T3 cells	PEG, Gd^{3+}	Liquid-phase exfoliation method	NIR, magnetic field	PTT, PA/MR imaging	200
	HeLa cells	/	Liquid exfoliation method	785 nm light	PTT	89
	HeLa cells, HepG2 cells	/	Hydrothermal method	NIR, X-ray	PTT, CT/PA imaging	201
WSe_2	HeLa cells, U14 cells	BSA, methylene blue	Liquid-phase exfoliation method	NIR	PTT + PDT	103

AlPc: aluminum phthalocyanine chloride; ATP: adenosine triphosphate; BSA: bovine serum albumin; Ce6: chlorin e6; CS: chitosan; CT: computed tomography; DOX: doxorubicin; FA: folic acid; FL: fluorescence; GSH: glutathione; GT: gene therapy; HA: hyaluronic acid; IONP: iron oxide nanoparticle; LA-K_{11}(DMA): LA-GKKKKKKKKKKK-NH_2(dimethylmaleic anhydride); MR: magnetic resonance; MSN: mesoporous silica nanoparticle; NIR: near-infrared; NIRF: near-infrared fluorescence; PA: photoacoustic; PANI: polyaniline; PDT: photodynamic therapy; PEG: polyethylene glycol; PEI: polyetherimide; PET: positron emission tomography; PLGA: poly(lactic-co-glycolic acid); PMO: periodic mesoporous organosilicas; POV: copolymer P(OEGA-co-VBA); PTT: photothermal therapy; PVP: poly(vinylpyrrolidone); RIT: radioisotope therapy; RT: radiotherapy.

combined in the therapeutic platforms. Thus, it is promising to further develop imaging-guided TMDC-based biocompatible nano-systems with both diagnostic and therapeutic functionalities.

In general, the development of stimuli-responsive TMDC nanomaterials is at a rapid rate but, it has not satisfied the demands in clinical applications up to now. More efforts are required on the unresolved issues to make more influencing progress in the future.

Conflicts of interest

There are no conflicts to declare.

Acknowledgements

This work was supported by the National Basic Research Program of China (Grant No. 2016YFA0201600), National Natural Science Foundation of China (Grant Nos. 51822207, 51772292, 31571015, 11621505, and 11435002), CAS Key Research Program of Frontier Sciences (Grant No. QYZDJ-SSW-SLH022), and Youth Innovation Promotion Association CAS (Grant No. 2013007).

Notes and references

1. S. Mura, J. Nicolas and P. Couvreur, *Nat. Mater.*, 2013, **12**, 991-1003.
2. R. Mo and Z. Gu, *Mater. Today*, 2016, **19**, 274-283.
3. V. P. Torchilin, *Adv. Drug Deliv. Rev.*, 2006, **58**, 1532-1555.

4. D. Peer, J. M. Karp, S. Hong, O. C. FaroKHzad, R. Margalit and R. Langer, *Nat. Nanotechnol.*, 2007, **2**, 751-760.
5. O. C. Farokhzad and R. Langer, *ACS Nano*, 2009, **3**, 16-20.
6. K. Yang, L. Feng and Z. Liu, *Adv. Drug Deliv. Rev.*, 2016, **105**, 228-241.
7. V. P. Torchilin, in *Stimuli-responsive Drug Delivery Systems*, The Royal Society of Chemistry, 2018, DOI: 10.1039/9781788013536-00001, pp. 1-32.
8. M. A. Stuart, W. T. Huck, J. Genzer, M. Muller, C. Ober, M. Stamm, G. B. Sukhorukov, I. Szleifer, V. V. Tsukruk, M. Urban, F. Winnik, S. Zauscher, I. Luzinov and S. Minko, *Nat. Mater.*, 2010, **9**, 101-113.
9. Y. L. Colson and M. W. Grinstaff, *Adv. Mater.*, 2012, **24**, 3878-3886.
10. E. Fleige, M. A. Quadir and R. Haag, *Adv. Drug Deliv. Rev.*, 2012, **64**, 866-884.
11. V. P. Torchilin, *Nat. Rev. Drug Discov.*, 2014, **13**, 813-827.
12. R. Cheng, F. Meng, C. Deng, H. A. Klok and Z. Zhong, *Biomaterials*, 2013, **34**, 3647-3657.
13. T. Liu, S. Shi, C. Liang, S. Shen, L. Cheng, C. Wang, X. Song, S. Goel, T. E. Barnhart, W. Cai and Z. Liu, *ACS Nano*, 2015, **9**, 950-960.
14. M. S. Shim and Y. J. Kwon, *Adv. Drug Deliv. Rev.*, 2012, **64**, 1046-1059.
15. S. Manzeli, D. Ovchinnikov, D. Pasquier, O. V. Yazyev and A. Kis, *Nat. Rev. Mater.*, 2017, **2**, 1-15.
16. M. Chhowalla, H. S. Shin, G. Eda, L. J. Li, K. P. Loh and H. Zhang, *Nat. Chem.*, 2013, **5**, 263-275.
17. X. Li, J. Shan, W. Zhang, S. Su, L. Yuwen and L. Wang, *Small*, 2017, **13**, 1602660.
18. X. Huang, Z. Zeng and H. Zhang, *Chem. Soc. Rev.*, 2013, **42**, 1934-1946.
19. K. Kalantar-zadeh, J. Z. Ou, T. Daeneke, M. S. Strano, M. Pumera and S. L. Gras, *Adv. Funct. Mater.*, 2015, **25**, 5086-5099.
20. B. Radisavljevic, A. Radenovic, J. Brivio, V. Giacometti and A. Kis, *Nat. Nanotechnol.*, 2011, **6**, 147-150.
21. S. Presolski and M. Pumera, *Mater. Today*, 2016, **19**, 140-145.
22. D. Chimene, D. L. Alge and A. K. Gaharwar, *Adv. Mater.*, 2015, **27**, 7261-7284.
23. R. Weissleder, *Nat. Biotechnol.*, 2001, **19**, 316-317.
24. T. Shao, J. Wen, Q. Zhang, Y. Zhou, L. Liu, L. Yuwen, Y. Tian, Y. Zhang, W. Tian and Y. Su, *J. Mater. Chem. B*, 2016, **4**, 7708-7717.
25. Z. Zhang, J. Wang and C. Chen, *Adv. Mater.*, 2013, **25**, 3869-3880.
26. R. Deng, H. Yi, F. Y. Fan, L. Fu, Y. Zeng, Y. Wang, Y. C. Li, Y. L. Liu, S. J. Ji and Y. Su, *RSC Adv.*, 2016, **6**, 77083-77092.
27. C. Wang, J. Bai, Y. W. Liu, X. D. Jia and X. Jiang, *ACS Biomater. Sci. Eng.*, 2016, **2**, 2011-2017.
28. W. Z. Teo, E. L. Chng, Z. Sofer and M. Pumera, *Chem. Eur. J.*, 2014, **20**, 9627-9632.
29. L. Gong, L. Yan, R. Zhou, J. Xie, W. Wu and Z. Gu, *J. Mater. Chem. B*, 2017, **5**, 1873-1895.
30. A. Gulzar, S. L. Gai, P. P. Yang, C. X. Li, M. B. Ansari and J. Lin, *J. Mater. Chem. B*, 2015, **3**, 8599-8622.
31. H. Li, Q. Zhang, C. C. R. Yap, B. K. Tay, T. H. T. Edwin, A. Olivier and D. Baillargeat, *Adv. Funct. Mater.*, 2012, **22**, 1385-1390.
32. T. Liu, Y. Chao, M. Gao, C. Liang, Q. Chen, G. S. Song, L. Cheng and Z. Liu, *Nano Research*, 2016, **9**, 3003-3017.
33. A. Zhang, A. Li, W. Zhao, G. Yan, B. Liu, M. Liu, M. Li, B. Huo and J. Liu, *Chem. Eng. J.*, 2018, **342**, 120-132.
34. Y. Yong, X. Cheng, T. Bao, M. Zu, L. Yan, W. Yin, C. Ge, D. Wang, Z. Gu and Y. Zhao, *ACS Nano*, 2015, **9**, 12451-12463.
35. S. Zhu, Z. Gu and Y. Zhao, *Adv. Therap.*, 2018, **1**, 1800050.
36. Y. Kato, S. Ozawa, C. Miyamoto, Y. Maehata, A. Suzuki, T. Maeda and Y. Baba, *Cancer Cell Int.*, 2013, **13**, 89.
37. P. Swietach, R. D. Vaughan-Jones, A. L. Harris and A. Hulikova, *Phil. Trans. R. Soc. B*, 2014, **369**, 20130099.
38. Z. Wang, X. Zhang, G. Huang and J. Gao, in *Stimuli-responsive Drug Delivery Systems*, The Royal Society of Chemistry, 2018, DOI: 10.1039/9781788013536-00051, pp. 51-82.
39. Y. Zhu and F. Chen, *Chem. Asian J.*, 2015, **10**, 284-305.
40. M. A. Keller, G. Piedrafita and M. Ralser, *Curr. Opin. Biotechnol.*, 2015, **34**, 153-161.
41. F. Q. Schafer and G. R. Buettner, *Free Radical Biol. Med.*, 2001, **30**, 1191-1212.
42. O. Zitka, S. Skalickova, J. Gumulec, M. Masarik, V. Adam, J. Hubalek, L. Trnkova, J. Kruseova, T. Eckschlager and R. Kizek, *Oncol. Lett.*, 2012, **4**, 1247-1253.
43. R. J. A. a. S. D. Roman, *Oxidative Med. Cell. Longev.*, 2008, **1**, 15-24.
44. Y. Li, K. Xiao, J. Luo, W. Xiao, J. S. Lee, A. M. Gonik, J. Kato, T. A. Dong and K. S. Lam, *Biomaterials*, 2011, **32**, 6633-6645.
45. Z. Gu, S. Zhu, L. Yan, F. Zhao and Y. Zhao, *Adv. Mater.*, 2019, **31**, e1800662.
46. A. Bhaw-Luximon and D. Jhurry, in *Stimuli-responsive Drug Delivery Systems*, The Royal Society of Chemistry, 2018, DOI: 10.1039/9781788013536-00109, pp. 109-144.
47. R. L. McCarley, *Annu. Rev. Anal. Chem. (Palo Alto Calif)*, 2012, **5**, 391-411.
48. R. Cheng, F. Feng, F. Meng, C. Deng, J. Feijen and Z. Zhong, *J. Control. Release*, 2011, **152**, 2-12.
49. Y. Xiong and K. L. Guan, *J. Cell Biol.*, 2012, **198**, 155-164.
50. E. Secret and J. S. Andrew, in *Stimuli-responsive Drug Delivery Systems*, The Royal Society of Chemistry, 2018, DOI: 10.1039/9781788013536-00209, pp. 209-231.
51. K. Kessenbrock, V. Plaks and Z. Werb, *Cell*, 2010, **141**, 52-67.
52. J. H. van Ree, K. B. Jeganathan, L. Malureanu and J. M. van Deursen, *J. Cell Biol.*, 2010, **188**, 83-100.
53. R. Jahanban-Esfahlan, M. de la Guardia, D. Ahmadi and B. Yousefi, *J. Cell. Physiol.*, 2018, **233**, 2019-2031.
54. P. Vaupel, K. Schlenger, C. Knoop and M. Hockel, *Cancer Res.*, 1991, **51**, 3316-3322.
55. S. A. P. a. M. C. S. Jessica A. Bertout, *Nat. Rev. Cancer*, 2008, **8**, 967-975.
56. L. L. Policastro, I. L. Ibanez, C. Notcovich, H. A. Duran and O. L. Podhajcer, *Antioxid. Redox Signal.*, 2013, **19**, 854-895.
57. A. L. Harris, *Nat. Rev. Cancer*, 2002, **2**, 38-47.
58. X. Li, J. Kim, J. Yoon and X. Chen, *Adv. Mater.*, 2017, **29**, 1606857.
59. M. G. Sikkandhar, A. M. Nedumaran, R. Ravichandar, S. Singh, I. Santhakumar, Z. C. Goh, S. Mishra, G. Archunan, B. Gulyas and P. Padmanabhan, *Int. J. Mol. Sci.*, 2017, **18**, 1036
60. T. Thambi, J. H. Park and D. S. Lee, *Chem. Commun.*, 2016, **52**, 8492-8500.
61. S. K. Jones, A. Sarkar, D. P. Feldmann, P. Hoffmann and O. M. Merkel, *Biomaterials*, 2017, **138**, 35-45.
62. L. C. Hartmann, G. L. Keeney, W. L. Lingle, T. J. Christianson, B. Varghese, D. Hillman, A. L. Oberg and P. S. Low, *Int. J. Cancer*, 2007, **121**, 938-942.
63. M. Hong, S. Zhu, Y. Jiang, G. Tang and Y. Pei, *J. Control. Release*, 2009, **133**, 96-102.
64. M. S. Shotaro Iwakiri, Shinjiro Nagai, Toshiki Hirata,Hiromi

Wada, and Ryo Miyahara, *Ann. Surg. Oncol.*, 2008, **15**, 889-899.

65. S. Xu, B. Z. Olenyuk, C. T. Okamoto and S. F. Hamm-Alvarez, *Adv. Drug Deliv. Rev.*, 2013, **65**, 121-138.
66. M. Karimi, A. Ghasemi, P. Sahandi Zangabad, R. Rahighi, S. M. Moosavi Basri, H. Mirshekari, M. Amiri, Z. Shafaei Pishabad, A. Aslani, M. Bozorgomid, D. Ghosh, A. Beyzavi, A. Vaseghi, A. R. Aref, L. Haghani, S. Bahrami and M. R. Hamblin, *Chem. Soc. Rev.*, 2016, **45**, 1457-1501.
67. J. Yao, J. Feng and J. Chen, *Asian J. Pharm. Sci.*, 2016, **11**, 585-595.
68. A. Jhaveri, P. Deshpande and V. Torchilin, *J. Control. Release*, 2014, **190**, 352-370.
69. X. Tan, E. L. Burchfield and K. Zhang, in *Stimuli-responsive Drug Delivery Systems*, The Royal Society of Chemistry, 2018, DOI: 10.1039/9781788013536-00163, pp. 163-191.
70. Q. Zhang, J. Zhang, S. Wan, W. Wang and L. Fu, *Adv. Funct. Mater.*, 2018, **28**, 1802500.
71. C. Oerlemans, W. Bult, M. Bos, G. Storm, J. F. Nijsen and W. E. Hennink, *Pharm. Res.*, 2010, **27**, 2569-2589.
72. T. J. Dougherty, C. J. Gomer, B. W. Henderson, D. K. Giulio Jori, M. Korbelik, J. Moan and Q. Peng, *J. Natl. Cancer Inst.*, 1998, **90**, 889-905.
73. A. Master, M. Livingston and A. Sen Gupta, *J. Control. Release*, 2013, **168**, 88-102.
74. E. Guisasola, A. Baeza and M. Vallet, in *Stimuli-responsive Drug Delivery Systems*, The Royal Society of Chemistry, 2018, DOI: 10.1039/9781788013536-00145, pp. 145-162.
75. W. Cheng, Y. Ping, Y. Zhang, K. H. Chuang and Y. Liu, *J. Healthc. Eng.*, 2013, **4**, 23-45.
76. P. Tartaj, M. D. Morales, S. Veintemillas-Verdaguer, T. Gonzalez-Carreno and C. J. Serna, *J. Phys. D-Appl. Phys.*, 2003, **36**, R182-R197.
77. I.Šafařík and M.Šafaříková, in *Nanostruct. Mater.*, SpringerWienNewYork, 2002, pp. 1-23.
78. R. K. Singh, K. D. Patel, J. J. Kim, T. H. Kim, J. H. Kim, U. S. Shin, E. J. Lee, J. C. Knowles and H. W. Kim, *ACS Appl. Mater. Interfaces*, 2014, **6**, 2201-2208.
79. J. Shi, X. Yu, L. Wang, Y. Liu, J. Gao, J. Zhang, R. Ma, R. Liu and Z. Zhang, *Biomaterials*, 2013, **34**, 9666-9677.
80. A. J. L. Villaraza, A. Bumb and M. W. Brechbiel, *Chem. Rev.*, 2010, **110**, 2921-2959.
81. P. Mi, D. Kokuryo, H. Cabral, M. Kumagai, T. Nomoto, I. Aoki, Y. Terada, A. Kishimura, N. Nishiyama and K. Kataoka, *J. Control. Release*, 2014, **174**, 63-71.
82. M. Sadeghi, M. Enferadi and A. Shirazi, *J. Canc. Res. Ther.*, 2010, **6**, 239-248.
83. M. Ma, Y. Huang, H. Chen, X. Jia, S. Wang, Z. Wang and J. Shi, *Biomaterials*, 2015, **37**, 447-455.
84. D. B. Chithrani, S. Jelveh, F. Jalali, M. van Prooijen, C. Allen, R. G. Bristow, R. P. Hill and D. A. Jaffray, *Radiat. Res.*, 2010, **173**, 719-728.
85. H. Wang, X. Mu, H. He and X. Zhang, *Trends Pharmacol. Sci.*, 2018, **39**, 24-48.
86. G. Qian, N. Wang, Q. Shen, Y. Sheng, J. Zhao, M. Kuang, G. Liu and M. Wu, *Eur. Radiol.*, 2012, **22**, 1983-1990.
87. A. Chilkoti, M. R. Dreher, D. E. Meyer and D. Raucher, *Adv. Drug Deliv. Rev.*, 2002, **54**, 613-630.
88. L. Chen, Y. Feng, X. Zhou, Q. Zhang, W. Nie, W. Wang, Y. Zhang and C. He, *ACS Appl. Mater. Interfaces*, 2017, **9**, 17347-17358.
89. L. Yuwen, J. Zhou, Y. Zhang, Q. Zhang, J. Shan, Z. Luo, L. Weng, Z. Teng and L. Wang, *Nanoscale*, 2016, **8**, 2720-2726.
90. S. Wang, K. Li, Y. Chen, H. Chen, M. Ma, J. Feng, Q. Zhao and J. Shi, *Biomaterials*, 2015, **39**, 206-217. DOI: 10.1039/C8TB03240H
91. X. Zhang, Z. Lai, Z. Liu, C. Tan, Y. Huang, B. Li, M. Zhao, L. Xie, W. Huang and H. Zhang, *Angew. Chem. Int. Ed. Engl.*, 2015, **54**, 5425-5428.
92. Q. Liu, C. Sun, Q. He, A. Khalil, T. Xiang, D. Liu, Y. Zhou, J. Wang and L. Song, *Nano Res.*, 2015, **8**, 3982-3991.
93. S. M. Lee, H. Park and K. H. Yoo, *Adv. Mater.*, 2010, **22**, 4049-4053.
94. X. Qian, S. Shen, T. Liu, L. Cheng and Z. Liu, *Nanoscale*, 2015, **7**, 6380-6387.
95. L. Chen, X. Zhou, W. Nie, W. Feng, Q. Zhang, W. Wang, Y. Zhang, Z. Chen, P. Huang and C. He, *ACS Appl. Mater. Interfaces*, 2017, **9**, 17786-17798.
96. X. Li, Y. Gong, X. Zhou, H. Jin, H. Yan, S. Wang and J. Liu, *Int. J. Nanomed.*, 2016, **11**, 1819-1833.
97. S. Ariyasu, J. Mu, X. Zhang, Y. Huang, E. K. L. Yeow, H. Zhang and B. Xing, *Bioconjugate Chem.*, 2017, **28**, 1059-1067.
98. Y. Liu and J. Liu, *Nanoscale*, 2017, **9**, 13187-13194.
99. X. Su, J. Wang, J. Zhang, L. Yuwen, Q. Zhang, M. Dang, J. Tao, X. Ma, S. Wang and Z. Teng, *J. Colloid Interface Sci.*, 2017, **496**, 261-266.
100. W. Liao, L. Zhang, Y. Zhong, Y. Shen, C. Li and N. An, *OncoTargets Ther.*, 2018, **11**, 1949-1960.
101. J. Lee, J. Kim and W. J. Kim, *Chem. Mater.*, 2016, **28**, 6417-6424.
102. G. Yang, H. Gong, T. Liu, X. Sun, L. Cheng and Z. Liu, *Biomaterials*, 2015, **60**, 62-71.
103. X. Jia, J. Bai, Z. Ma and X. Jiang, *J. Mater. Chem. B*, 2017, **5**, 269-278.
104. Y. Yong, L. Zhou, Z. Gu, L. Yan, G. Tian, X. Zheng, X. Liu, X. Zhang, J. Shi, W. Cong, W. Yin and Y. Zhao, *Nanoscale*, 2014, **6**, 10394-10403.
105. S. S. Chou, B. Kaehr, J. Kim, B. M. Foley, M. De, P. E. Hopkins, J. Huang, C. J. Brinker and V. P. Dravid, *Angew. Chem. Int. Ed. Engl.*, 2013, **52**, 4160-4164.
106. L. Cheng, J. Liu, X. Gu, H. Gong, X. Shi, T. Liu, C. Wang, X. Wang, G. Liu, H. Xing, W. Bu, B. Sun and Z. Liu, *Adv. Mater.*, 2014, **26**, 1886-1893.
107. W. Yin, L. Yan, J. Yu, G. Tian, L. Zhou, X. Zheng, X. Zhang, Y. Yong, J. Li, Z. Gu and Y. Zhao, *ACS Nano*, 2014, **8**, 6922-6933.
108. T. Liu, C. Wang, W. Cui, H. Gong, C. Liang, X. Shi, Z. Li, B. Sun and Z. Liu, *Nanoscale*, 2014, **6**, 11219-11225.
109. K. Dong, Z. Liu, Z. Li, J. Ren and X. Qu, *Adv. Mater.*, 2013, **25**, 4452-4458.
110. K. L. O'Neill, D. W. Fairbairn, M. J. Smith and B. S. Poe, *Apoptosis*, 1998, **3**, 369-375.
111. C. Chen, L. Zhou, J. Geng, J. Ren and X. Qu, *Small*, 2013, **9**, 2793-2800.
112. R. K. PANDEY, *J. Porphyr. Phthalocyanines*, 1999, **4**, 368-373.
113. S. S. Lucky, K. C. Soo and Y. Zhang, *Chem. Rev.*, 2015, **115**, 1990-2042.
114. L. Liu, J. Wang, Q. You, Q. Sun, Y. Song, Y. Wang, Y. Cheng, S. Wang, F. Tan and N. Li, *J. Mater. Chem. B*, 2018, **6**, 4239-4250.
115. M. Peng, D. Zheng, S. Wang, S. Cheng and X. Zhang, *ACS Appl. Mater. Interfaces*, 2017, **9**, 13965-13975.
116. S. P. Sherlock, S. M. Tabakman, L. Xie and H. Dai, *ACS Nano*, 2011, **5**, 1505-1512.
117. J. H. Sayda M. Elbashir, Winfried Lendeckel, Abdullah Yalcin, Klaus Weber & Thomas Tuschl, *Nature*, 2001, **411**, 494-498.
118. P. D. Zamore, *Cell*, 2006, **127**, 1083-1086.
119. J. C. Burnett and J. J. Rossi, *Chem. Biol.*, 2012, **19**, 60-71.

120. J. A. Kemp, M. S. Shim, C. Y. Heo and Y. J. Kwon, *Adv. Drug Deliv. Rev.*, 2016, **98**, 3-18.
121. H. Dong, W. Dai, H. Ju, H. Lu, S. Wang, L. Xu, S. F. Zhou, Y. Zhang and X. Zhang, *ACS Appl. Mater. Interfaces*, 2015, **7**, 11015-11023.
122. F. Yin, K. Hu, Y. Chen, M. Yu, D. Wang, Q. Wang, K. T. Yong, F. Lu, Y. Liang and Z. Li, *Theranostics*, 2017, **7**, 1133-1148.
123. C. Zhang, Y. Yong, L. Song, X. Dong, X. Zhang, X. Liu, Z. Gu, Y. Zhao and Z. Hu, *Adv. Healthc. Mater.*, 2016, **5**, 2776-2787.
124. J. T. Douglas, *Technol. Cancer Res. Treat.*, 2003, **2**, 51-64.
125. T. Wirth and S. Yla-Herttuala, *Biomedicines*, 2014, **2**, 149-162.
126. J. Kim, H. Kim and W. J. Kim, *Small*, 2016, **12**, 1184-1192.
127. N. Ballatori, S. M. Krance, S. Notenboom, S. Shi, K. Tieu and C. L. Hammond, *Biol. Chem.*, 2009, **390**, 191-214.
128. S. Chen, C. Lin, T. Cheng and W. Tseng, *Adv. Funct. Mater.*, 2017, **27**, 1702452.
129. T. K. Nguyen, R. Selvanayagam, K. K. K. Ho, R. Chen, S. K. Kutty, S. A. Rice, N. Kumar, N. Barraud, H. T. T. Duong and C. Boyer, *Chem. Sci.*, 2016, **7**, 1016-1027.
130. S. Sarkar, V. I. Korolchuk, M. Renna, S. Imarisio, A. Fleming, A. Williams, M. Garciaarencibia, C. Rose, S. Luo and B. R. Underwood, *Mol. Cell*, 2011, **43**, 19-32.
131. Q. Gao, X. Zhang, W. Yin, D. Ma, C. Xie, L. Zheng, X. Dong, L. Mei, J. Yu, C. Wang, Z. Gu and Y. Zhao, *Small*, 2018, **14**, 1802290.
132. J. B. Mitchell, D. A. Wink, W. DeGraff, J. Gamson, L. K. Keefer and M. C. Krishna, *Cancer Res.*, 1993, **53**, 5845-5848.
133. J. Bourassa, W. DeGraff, S. Kudo, D. A. Wink, J. B. Mitchell and P. C. Ford, *J. Am. Chem. Soc.*, 1997, **119**, 2853-2860.
134. Q. Song, S. Tan, X. Zhuang, Y. Guo, Y. Zhao, T. Wu, Q. Ye, L. Si and Z. Zhang, *Mol. Pharm.*, 2014, **11**, 4118-4129.
135. X. Zhang, G. Tian, W. Yin, L. Wang, X. Zheng, L. Yan, J. Li, H. Su, C. Chen, Z. Gu and Y. Zhao, *Adv. Funct. Mater.*, 2015, **25**, 3049-3056.
136. K. Zhang, H. Xu, X. Jia, Y. Chen, M. Ma, L. Sun and H. Chen, *ACS Nano*, 2016, **10**, 10816-10828.
137. X. Zhang, Z. Guo, J. Liu, G. Tian, K. Chen, S. Yu and Z. Gu, *Sci. Bull.*, 2017, **62**, 985-996.
138. M. M. Gottesman, *Annu. Rev. Med.*, 2002, **53**, 615-627.
139. S. Wang, Y. Chen, X. Li, W. Gao, L. Zhang, J. Liu, Y. Zheng, H. Chen and J. Shi, *Adv. Mater.*, 2015, **27**, 7117-7122.
140. X. He, J. Li, S. An and C. Jiang, *Ther. Deliv.*, 2013, **4**, 1499-1510.
141. M. Stubbs, P. M. J. McSheehy, J. R. Griffiths and C. L. Bashford, *Mol. Med. Today*, 2000, **6**, 15-19.
142. J. Yu, X. Chu and Y. Hou, *Chem. Commun.*, 2014, **50**, 11614-11630.
143. Q. Huang, S. Wang, J. Zhou, X. Zhong and Y. Huang, *RSC Adv.*, 2018, **8**, 4624-4633.
144. T. Liu, C. Wang, X. Gu, H. Gong, L. Cheng, X. Shi, L. Feng, B. Sun and Z. Liu, *Adv. Mater.*, 2014, **26**, 3433-3440.
145. C. H. Park, S. Lee, G. Pornnoppadol, Y. S. Nam, S. H. Kim and B. J. Kim, *ACS Appl. Mater. Interfaces*, 2018, **10**, 9023-9031.
146. Q. Lei, S. Wang, J. Hu, Y. Lin, C. Zhu, L. Rong and X. Zhang, *ACS Nano*, 2017, **11**, 7201-7214.
147. A. Zhang, A. Li, W. Tian, Z. Li, C. Wei, Y. Sun, W. Zhao, M. Liu and J. Liu, *Chem. Eur. J.*, 2017, **23**, 11346-11356.
148. W. Zhao, A. Li, C. Chen, F. Quan, L. Sun, A. Zhang, Y. Zheng and J. Liu, *J. Mater. Chem. B*, 2017, **5**, 7403-7414.
149. X. Dong, W. Yin, X. Zhang, S. Zhu, X. He, J. Yu, J. Xie, Z. Guo, L. Yan, X. Liu, Q. Wang, Z. Gu and Y. Zhao, *ACS Appl. Mater. Interfaces*, 2018, **10**, 4271-4284.
150. S. H. Yun and S. J. J. Kwok, *Nat. Biomed. Eng*, 2017, **1**, 1-16.
151. K. Brindle, *Nat. Rev. Cancer*, 2008, **8**, 94-107.
152. R. Weissleder and M. J. Pittet, *Nature*, 2008, **452**, 580-589.
153. P. Caravan, J. J. Ellison, T. J. McMurry and R. B. Lauffer, *Chem. Rev.*, 1999, **99**, 2293-2352.
154. W. Lin, T. Hyeon, G. M. Lanza, M. Zhang and T. J. Meade, *MRS Bull.*, 2009, **34**, 441-448.
155. K. M. L. Taylor, J. S. Kim, W. J. Rieter, H. An, W. Lin and W. Lin, *J. Am. Chem. Soc.*, 2007, **130**, 2154-2155.
156. O. T. B. Ulrich I. Tromsdorf, Sunhild C. Salmen, Ulrike Beisiegel, and Horst Weller, *Nano Lett.*, 2009, **9**, 4434-4440.
157. J. L. Major and T. J. Meade, *Acc. Chem. Res.*, 2009, **42**, 893-903.
158. W. Xie, Q. Gao, D. Wang, Z. H. Guo, F. Gao, X. Wang, Q. Cai, S. Feng, H. Fan, X. Sun and L. Zhao, *Nano Res.*, 2018, **11**, 2470-2487.
159. R. Anbazhagan, Y. Su, H. Tsai and R. Jeng, *ACS Appl. Mater. Interfaces*, 2016, **8**, 1827-1835.
160. Y. Chen, L. Cheng, Z. Dong, Y. Chao, H. Lei, H. Zhao, J. Wang and Z. Liu, *Angew. Chem. Int. Ed. Engl.*, 2017, **56**, 12991-12996.
161. J. Yu, W. Yin, X. Zheng, G. Tian, X. Zhang, T. Bao, X. Dong, Z. Wang, Z. Gu, X. Ma and Y. Zhao, *Theranostics*, 2015, **5**, 931-945.
162. H. Wang, Z. Zeng, T. Bui, S. DiBiase, W. Qin, F. Xia, S. Powell and G. Iliakis, *Cancer Res.*, 2001, **61**, 270-277.
163. T. W. Meijer, J. H. Kaanders, P. N. Span and J. Bussink, *Clin. Cancer. Res.*, 2012, **18**, 5585-5594.
164. W. Fan, B. Yung, P. Huang and X. Chen, *Chem. Rev.*, 2017, **117**, 13566-13638.
165. J. Wang, X. Pang, X. Tan, Y. Song, L. Liu, Q. You, Q. Sun, F. Tan and N. Li, *Nanoscale*, 2017, **9**, 5551-5564.
166. Y. Chao, G. Wang, C. Liang, X. Yi, X. Zhong, J. Liu, M. Gao, K. Yang, L. Cheng and Z. Liu, *Small*, 2016, **12**, 3967-3975.
167. L. Cheng, C. Yuan, S. Shen, X. Yi, H. Gong, K. Yang and Z. Liu, *ACS Nano*, 2015, **9**, 11090-11101.
168. S. Shen, Y. Chao, Z. Dong, G. Wang, X. Yi, G. Song, K. Yang, Z. Liu and L. Cheng, *Adv. Funct. Mater.*, 2017, **27**, 1700250.
169. J. Wang, X. Tan, X. Pang, L. Liu, F. Tan and N. Li, *ACS Appl. Mater. Interfaces*, 2016, **8**, 24331-24338.
170. S. Wang, X. Li, Y. Chen, X. Cai, H. Yao, W. Gao, Y. Zheng, X. An, J. Shi and H. Chen, *Adv. Mater.*, 2015, **27**, 2775-2782.
171. W. Chen, R. L. Adams, R. Carubelli and R. E. Nordquist, *Cancer Lett.*, 1997, **115**, 25-30.
172. P. R. M. Stephen M. Waldow, and Leonard I. Grossweiner, *Lasers Surg. Med.*, 1988, **8**, 510-514.
173. T. S. M. Castren-Persons, O.J. Ramo, P. Puolakkainen, and E. Lehtonen, *Lasers Surg. Med.*, 1991, **11**, 595-600.
174. E. S. Day, J. G. Morton and J. L. West, *J. Biomech. Eng.-Trans. ASME*, 2009, **131**, 074001.
175. C. Oliver Kappe, *Chem. Soc. Rev.*, 2008, **37**, 1127-1139.
176. M. T. Ken Motokura, and Yasuhiro Iwasawa, *J. Am. Chem. Soc.*, 2008, **131**, 7944–7945.
177. K. Raidongia and J. Huang, *J. Am. Chem. Soc.*, 2012, **134**, 16528-16531.
178. X. Zheng, J. Xu, K. Yan, H. Wang, Z. Wang and S. Yang, *Chem. Mater.*, 2014, **26**, 2344-2353.
179. C. O. Kappe, *Angew. Chem. Int. Ed. Engl.*, 2004, **43**, 6250-6284.
180. S. Wang, L. Tan, P. Liang, T. Liu, J. Wang, C. Fu, J. Yu, J. Dou, L. Hong and X. Meng, *J. Mater. Chem. B*, 2016, **4**, 2133-2141.
181. S. Tang, C. Fu, L. Tan, T. Liu, J. Mao, X. Ren, H. Su, D. Long, Q. Chai, Z. Huang, X. Chen, J. Wang, J. Ren and X. Meng, *Biomaterials*, 2017, **133**, 144-153.

View Article Online
DOI: 10.1039/C8TB03240H

182. C. Fu, F. He, L. Tan, X. Ren, W. Zhang, T. Liu, J. Wang, J. Ren, X. Chen and X. Meng, *Nanoscale*, 2017, **9**, 14846-14853.
183. J. N. Coleman, M. Lotya, A. O'Neill, S. D. Bergin, P. J. King, U. Khan, K. Young, A. Gaucher, S. De, R. J. Smith, I. V. Shvets, S. K. Arora, G. Stanton, H. Y. Kim, K. Lee, G. T. Kim, G. S. Duesberg, T. Hallam, J. J. Boland, J. J. Wang, J. F. Donegan, J. C. Grunlan, G. Moriarty, A. Shmeliov, R. J. Nicholls, J. M. Perkins, E. M. Grieveson, K. Theuwissen, D. W. McComb, P. D. Nellist and V. Nicolosi, *Science*, 2011, **331**, 568-571.
184. R. J. Smith, P. J. King, M. Lotya, C. Wirtz, U. Khan, S. De, A. O'Neill, G. S. Duesberg, J. C. Grunlan, G. Moriarty, J. Chen, J. Wang, A. I. Minett, V. Nicolosi and J. N. Coleman, *Adv. Mater.*, 2011, **23**, 3944-3948.
185. Z. Zeng, Z. Yin, X. Huang, H. Li, Q. He, G. Lu, F. Boey and H. Zhang, *Angew. Chem. Int. Ed. Engl.*, 2011, **50**, 11093-11097.
186. B. L. Li, M. I. Setyawati, L. Chen, J. Xie, K. Ariga, C. T. Lim, S. Garaj and D. T. Leong, *ACS Appl. Mater. Interfaces*, 2017, **9**, 15286-15296.
187. L. Kong, L. Xing, B. Zhou, L. Du and X. Shi, *ACS Appl. Mater. Interfaces*, 2017, **9**, 15995-16005.
188. C. Song, C. Yang, F. Wang, D. Ding, Y. Gao, W. Guo, M. Yan, S. Liu and C. Guo, *J. Mater. Chem. B*, 2017, **5**, 9015-9024.
189. L. Liu, J. Wang, X. Tan, X. Pang, Q. You, Q. Sun, F. Tan and N. Li, *J. Mater. Chem. B*, 2017, **5**, 2286-2296.
190. L. Jia, L. Ding, J. Tian, L. Bao, Y. Hu, H. Ju and J. S. Yu, *Nanoscale*, 2015, **7**, 15953-15961.
191. X. D. Meng, Z. Q. Liu, Y. Cao, W. H. Dai, K. Zhang, H. F. Dong, X. Y. Feng and X. J. Zhang, *Adv. Funct. Mater.*, 2017, **27**, 1605592.
192. X. Jing, Z. Zhi, D. Wang, J. Liu, Y. Shao and L. Meng, *Bioconjugate Chem.*, 2018, **29**, 559-570.
193. C. Wu, J. Zhao, F. Hu, Y. Zheng, H. Yang, S. Pan, S. Shi, X. Chen and S. Wang, *Carbohydr. Polym.*, 2018, **180**, 112-121.
194. S. Wang, J. Zhao, H. Yang, C. Wu, F. Hu, H. Chang, G. Li, D. Ma, D. Zou and M. Huang, *Acta Biomater.*, 2017, **58**, 442-454.
195. Z. H. Miao, L. X. Lv, K. Li, P. Y. Liu, Z. Li, H. Yang, Q. Zhao, M. Chang, L. Zhen and C. Y. Xu, *Small*, 2018, **14**, e1703789.
196. Y. Liu, X. Ji, J. Liu, W. W. L. Tong, D. Askhatova and J. Shi, *Adv. Funct. Mater.*, 2017, **27**, 1703261
197. Z. Lei, W. Zhu, S. Xu, J. Ding, J. Wan and P. Wu, *ACS Appl. Mater. Interfaces*, 2016, **8**, 20900-20908.
198. J. Chen, X. Li, X. Liu, H. Yan, Z. Xie, Z. Sheng, X. Gong, L. Wang, X. Liu, P. Zhang, H. Zheng, L. Song and C. Liu, *Biomater Sci*, 2018, **6**, 1503-1516.
199. C. L. Zhong, X. Zhao, L. J. Wang, Y. X. Li and Y. Y. Zhao, *Rsc Advances*, 2017, **7**, 7382-7391.
200. J. Pan, X. Zhu, X. Chen, Y. Zhao and J. Liu, *Biomater Sci*, 2018, **6**, 372-387.
201. B. Mao, T. Bao, J. Yu, L. Zheng, J. Qin, W. Yin and M. Cao, *Nano Research*, 2017, **10**, 2667-2682.

View Article Online
DOI: 10.1039/C8TB03240H

TOC:

A comprehensive overview of the development of stimuli-responsive TMDC-based nanoplatforms for "smart" cancer therapy is presented to demonstrate a more intelligent and better controllable therapeutic strategy.